2022

Cranial morphology of the Stellate Sturgeon, Acipenser stellatus Pallas 1771 (Acipenseriformes, Acipenseridae), with notes on the skulls of other sturgeons

Eric J. Hilton
Virginia Institute of Marine Science

Casey B. Dillman

Marian Paraschiv

Radu Suciu

Recommended Citation

Hilton, Eric J.; Dillman, Casey B.; Paraschiv, Marian; and Suciu, Radu, Cranial morphology of the Stellate Sturgeon, Acipenser stellatus Pallas 1771 (Acipenseriformes, Acipenseridae), with notes on the skulls of other sturgeons (2022). *Acta zoologica*, 1036(1), 57-77.
doi: 10.1111/azo.12355

DR ERIC HILTON (Orcid ID : 0000-0003-1742-3467)

Article type : Original Manuscript

Cranial morphology of the Stellate Sturgeon, *Acipenser stellatus* Pallas 1771 (Acipenseriformes, Acipenseridae), with notes on the skulls of other sturgeons

Eric J. Hilton[1], Casey B. Dillman[2], Marian Paraschiv[3], and Radu Suciu[4]

[1]Virginia Institute of Marine Science, William & Mary, Gloucester Point, VA 23062, U.S.A.; ehilton@vims.edu

[2]Cornell University Museum of Vertebrates, Department of Ecology and Evolutionary Biology, Cornell University, Ithaca, NY 14850, U.S.A; cbd63@cornell.edu

[3]Danube Delta National Institute, Tulcea, 820112, Romania; marian.paraschiv@ddni.ro

[4]Suciu I.E. Radu PFA. 827978 Telița, Romania; radu.suciu34@gmail.com

Keywords: Actinopterygii; comparative anatomy; osteology

Abstract

Hilton, E.J., Dillman, C.B., Paraschiv, M., and Suciu, R. Cranial morphology of the Stellate Sturgeon, *Acipenser stellatus* Pallas 1771 (Acipenseriformes, Acipenseridae), with notes on the skulls of other sturgeons — Acta Zoologica (Stockholm)

Extant members of Acipenseridae are generally classified in four genera: *Scaphirhynchus*, *Pseudoscaphirhynchus*, *Huso,* and "*Acipenser,*" which is widely-recognized to be paraphyletic. Advances have been made in understanding the systematic relationships among sturgeons based on both morphological and molecular data. Analysis of mitochondrial DNA data suggested that *Pseudoscaphirhynchus* should be regarded as nested within "*Acipenser,*" specifically as sister-group to the Stellate Sturgeon, *A. stellatus*. Recent morphological analyses also recovered this relationship, supported by a number of osteological synapomorphies, although these results were based on few and relatively small individuals. Here we describe the anatomy of the skull of *A. stellatus* based on newly prepared specimens of adult individuals, as well as examination of a large number of preserved individuals representing a broad range of ontogenetic stages. We present new anatomical data from all regions of the skull (dermatocranium, neurocranium, viscerocranium) and offer interpretations of these and other characters. In particular, we describe the allometry in the snout of *A. stellatus*, which undergoes substantial elongation relative to other sturgeons. Aspects of the skull of *A. stellatus* are compared to other members of the family, specifically the course of the occipital sensory canal and the morphology and distribution of cranial spines.

Eric J. Hilton, Department of Fisheries Science, Virginia Institute of Marine Science, William & Mary, Gloucester Point, VA 23062, USA. E-mail: ehilton@vims.edu

Introduction

Morphological and anatomical studies of sturgeons (Acipenseriformes, Acipenseridae) have enjoyed a long history, due in part to the "archaic" appearance of these fishes and their phylogenetic position at the base of Actinopterygii, the ray-finned fishes (Bemis et al., 1997; Hilton et al., 2011). The family currently includes approximately 25 extant species placed in four broadly recognized genera (*Acipenser*, *Huso*, *Pseudoscaphirhynchus*, and *Scaphirhynchus*). The oldest fossil remains of the family (Santonian Age) are highly fragmentary (e.g., isolated and fragmentary scutes and spines), and largely undiagnosable beyond the family level (Hilton and Grande, 2006; Kolvachuk and Hilton, 2017), although there are a few fossil taxa known from whole-body specimens (e.g., †*Priscosturion*, Grande and Hilton, 2006, 2009; †*Anchiacipenser*, Sato et al., 2018; two undescribed Late Cretaceous taxa currently under study by E. J. Hilton and

L. Grande). Extant sturgeons are characterized by having five rows of bony plates (scutes) along the length of their body (organized as a median dorsal, and paired lateral and ventral rows), robust bony pectoral-fin spines, and strongly heterocercal caudal fins. Despite these obvious characters uniting the family, which represent a mixture of plesiomorphic and apomorphic features and give these fishes a stereotyped bauplan, there is substantial phenotypic variation within the group that has generated myriad phylogenetic hypotheses. Given the alternate hypotheses of relationships within the family, even basic questions such as the monophyly of *Acipenser*, the most species-rich genus of the family, remain contentious.

One example of this phylogenetic unrest relates to the position of genus *Pseudoscaphirhynchus* from the tributaries of the Aral Sea. The three recognized species of this genus, each with diagnosable morphs (Kuhajda, 2002) have traditionally been aligned with the North American river sturgeons, genus *Scaphirhynchus* (although see Mayden and Kuhajda, 1996, who recovered the genus as a paraphyletic grade sister to *Scaphirhynchus*). This sister-group relationship was formalized in the classification of Findeis (1997) as the tribe Scaphirhynchini based on characters of the neurocranium, dermal skull roof, jaws and hyoid skeleton, and caudal skeleton (see also characters cited in Mayden and Kuhajda, 1996). This traditionally accepted group has been challenged on both molecular (Birstein et al., 2002; Dillman et al., 2007; Kreiger et al., 2008) and morphological grounds (Hilton, 2005; Hilton et al., 2011). Birstein et al. (2002), using sequence data from five mitochondrial loci recovered a very strongly-supported sister group relationship between *Pseudoscaphirhynchus* and *A. stellatus*. Dillman et al. (2007) and Krieger et al. (2008), based on additional mitochondrial data, also recovered a sister-group relationship between these taxa. Hilton (2005) described morphological evidence consistent with this hypothesis (i.e., *Pseudoscaphirhynchus* + *A. stellatus*). Hilton et al. (2011) tested this hypothesis in a morphological examination of the Acipenseridae. The clade was found to be united by a single unambiguous synapomorphy, the horizontal arm of the jugal bone undercutting the nasal capsule (character 7, state 1; Hilton et al., 2011). This clade is further supported, though not unambiguously, by spines on the dermal skull bones (character 13; state 1), the absence of the medial process of the jugal (character 8; state 1), and the trunk occipital and supraorbital lateral lines meeting in the lateral extrascapular (character 14; state 1). The skeletal anatomy of sturgeons continues to be investigated and has been reassessed in a series of recent studies to add to the body of morphological information about these fishes. These studies

have been approached from descriptive and phylogenetic perspectives (Hilton, 2005; Hilton et al., 2011; Hilton and Bemis, 2012; Hilton et al., 2016) and ontogenetic perspectives (Dillman and Hilton, 2015; Warth et al., 2017, 2018). From these studies it is clear that much is still to be learned about the internal relationships of the family, for which a better understanding of their morphology is necessary. However, anatomical data for several key taxa, including *A. stellatus*, are lacking.

The Stellate Sturgeon, *Acipenser stellatus* (Fig. 1), is a relatively small species of sturgeon, with a maximum known size of 218 cm total length and a weight of 54 kg (Borzenko, 1942, cited in Shubina et al., 1989). *Acipenser stellatus*, together with other species of sturgeons such as *H. huso*, *A. ruthenus*, *A. sturio*, *S. platorhynchus*, and *Pseudoscaphirhynchus kaufmanni*, is a member of the so-called 120-chromosome group of sturgeons (Group A of Fontana, 2002; see also Kovalev et al., 2014 for *P. kaufmanni*), with a karyotype of $2n = 146 \pm 6$; 37 pairs of meta-submetacentric chromosomes, the balance are acrocentrics and microchromosomes (Chicca et al. 2002; see also Birstein and Vasil'ev, 1987, Suciu and Ene, 1996, and Nowruzfashkhami and Khosroshahi, 1999, who estimated different numbers of chromosomes in this species using different methodologies). *Acipenser stellatus* is anadromous and occurs throughout the Black, Agean, Caspian, and Asov seas and the major tributaries of these waters; introductions were made also to the Aral Sea but these appear to be unsuccessful (Shubina et al. 1989). It feeds primarily on invertebrates and fishes. In the Caspian Sea, *A. stellatus* feed primarily on *Neogobius* sp. (Gobiidae) and bivalve mollusks (Cardiidae and Scrobiculariidae) when measured as both percent abundance and percent occurrence, although there is seasonal variation in diet (Naderi et al., 2016). Juveniles feed in the Danube River estuary until they are 3 to 4 years old (Holostenco et al., 2013). As adults, they make long migrations to spawning grounds (Kynard et al., 2002). In the Danube River, some individuals enter the river in the late summer or early fall to overwinter in the river; these individuals presumably migrate further upstream to spawning grounds than those individuals that migrate into the river in the spring (Honţ et al., 2019). One acoustically tagged individual was repeatedly recorded near the Iron Gate II dam, trying for 11 days to pass upstream of the dam. This was suggested to reflect homing fidelity of a fish originating from parents born upstream before the construction of the dam (Honţ et al. 2019). In a population genetic study of sturgeons in the Danube Delta Biosphere Reserve, the haplotype diversity of *A. stellatus* was greater in the Lower Danube River than in the coastal portion of the

Black Sea, with regional differences in diversity within the Black Sea (Holostenco et al., 2013). The species has experienced significant declines in population sizes due to natural (e.g., river discharge) and anthropogenic (dams, pollution, and illegal fishing) factors, and is considered Endangered by IUCN (Vecsei et al., 2001, 2007; Suciu and Guti, 2012; Friedrich, 2018, Ruban et al., 2019).

Four subspecies of *Acipenser stellatus* have been described across its expansive Ponto-Caspian range (Fricke et al., 2020). These forms were based on aspects of their head morphology, although none are currently regarded as valid and possibly reflect environmental and habitat differences (e.g., between the Sea of Asov and the Caspian Sea; Shubina et al., 1989). *Acipenser stellatus* is readily identifiable from all other sturgeon by a combination of an exceptionally long, narrow snout (unique among extant taxa), a relatively slender pectoral fin spine, and the presence of moderately sized bony plates intercalated between the dorsal and lateral rows of scutes (other species variably possess these plates as well). Most anatomical data that are available for *A. stellatus* relate to its external morphology (Fitzinger and Heckel 1836; Heckel and Kner, 1858; Antipa, 1909; Antoniu Murgoci, 1937a; Borzenko 1942; Berg, 1948, Holcik, 1959; summarized by Shubina et al., 1989 and Vecsei et al., 2007). Relatively little information is available for the skeletal anatomy of *Acipenser stellatus*, with the most comprehensive series of studies completed by Antoniu Murgoci (1937a, b; 1942). In a largely overlooked paper, Kittary (1850) described the skull of *A. stellatus* in comparison to other species of Caspian Sea sturgeon. Bakhshalizadeh et al. (2013: 474) compared the pectoral-fin spine of *A. stellatus*, which was characterized as "thin, serrated on the external side, and forked distally," to that of other sturgeons from the Caspian Sea. Hilton (2005) compared the bones of the skull roof of *A. stellatus* to those of *Pseudoscaphirhynchus*. The goal of this paper is to contribute new data on the cranial anatomy of *Acipenser stellatus*. We revisit the cranial morphology of *A. stellatus*, building upon the preliminary observations made by Hilton (2005, also Hilton et al. 2011). Here we describe the skull of *A. stellatus* based on newly prepared adult specimens, a life history stage that was not available to Hilton (2005). These new observations are compared to other sturgeons and in reference to recent phylogenetic hypotheses of sturgeons.

Materials and Methods

Specimens of *Acipenser stellatus* were dissected fresh at the Danube Delta National Institute (Tulcea, Romania) in November 2011, and prepared as dry skeletons following methods outlined in Bemis et al. (2004) and Hilton et al. (2011). New specimens of additional taxa were also prepared for comparisons. Cleared and stained specimens of juveniles prepared following protocols modified from Dingerkus and Uhler (1977) were also examined. Institutional abbreviations follow Sabaj (2019).

In addition to the newly prepared specimens, preserved museum specimens were examined to collect morphometric data (Fig. 2). Measurements include: Standard Length (SL, from anterior tip of snout to posteriormost keeled lateral scute); Head Length (HL, from anterior tip of snout to posterior margin of the subopercle); Preorbital Length (from anterior tip of snout to anterior margin of orbit); Prenares Length (from anterior tip of snout to anterior margin of the anterior nares); Preoral Length (from anterior tip of snout to anterior tip of upper jaw when retracted); Prebarbel Length (from anterior tip of snout to the anteriormost barbel); Skull Width at Opercular Flap (width of skull at the dorsal insertion of the fleshy extension along the posterior margin of the opercular elements, i.e., the subopercle and branchiostegal); Interorbital Width (width of the skull at dorsal midpoint of orbit); Head Width at Nares and Barbels (width of head at level of respective structure); Mouth Width (mouth width inside of jaws; i.e., excluding fleshy lips); Head Height at Opercular Flap, Orbit, Nares, and Barbel (height of head at level of respective structure). Specimens that were obviously damaged were excluded from measurements for those structures that were affected by the damage.

Specimens examined (SL, is given; TL or HL is given if SL is not known)

Acipenser stellatus: MNHN 1997-4163, 180 mm SL; MNHN 1997-4166, 402 mm SL; MNHN 1997-4167, 227 mm SL; MNHN 1997-4167, 390 mm SL; MNHN 5156, 665 mm SL; UMMZ 184980, 112 mm SL; VIMS 42686, 27.5 mm TL; VIMS 42687, 30.5 mm TL; VIMS 42688, 38.0 mm TL; VIMS 42689, 37.5 mm TL; VIMS 42690, 32.0 mm TL; VIMS 13552, 235 mm HL; VIMS 13553, 320 mm HL; ZIN 13752, 442 mm SL; ZIN 14557, 543 mm SL; ZIN 15027, 341 mm SL; ZIN 15027, 455 mm SL; ZIN 34908, 286 mm SL; ZIN 34908, 385 mm SL; ZIN 34908, 391 mm SL; ZIN 35749, 56 mm SL; ZIN 35750, 55 mm SL; ZIN 35750, 62 mm SL; ZIN 36347, 181 mm SL; ZIN 47526, 114 mm SL; ZIN 47526, 158 mm SL; ZIN 47526, 164 mm SL; ZIN 47526, 178 mm SL; ZIN 47526, 213 mm SL; ZIN 47526, 228 mm SL; ZIN 7717, 244 mm SL;

ZIN 7717, 292 mm SL; ZIN 7717, 375 mm SL; ZMMU 17307, 275 mm SL; ZMMU 17307, 280 mm SL; ZMMU 17307, 311 mm SL; ZMMU 17307, 330 mm SL; ZMMU 17307, 350 mm SL; ZMMU 1984, 101 mm SL; ZMMU 1984, 160 mm SL; ZMMU 1984, 202 mm SL; ZMMU 22290, 195 mm SL; ZMMU 22290, 223 mm SL; ZMMU 22290, 365 mm SL; ZMMU 22290, 400 mm SL.

Specimens of other members of Acipenseridae listed in Hilton (2005) and Hilton et al. (2011) were also examined; additional specimens examined are cited in text.

Results

General morphology and shape of the head

Table 1 presents selected variables describing the shape and variation of the head in *Acipenser stellatus*. In general, the head of *A. stellatus* is much longer and narrower than that of other species of sturgeon (Shubina et al., 1989), although at early stages of ontogeny, the head does not show this specialization. In larvae and small juveniles (e.g., <30 mm SL), the head is approximately triangular in dorsal view, with a sharply pointed snout (Fig. 3A-C). In larger juveniles and adults, the snout is longer. It bears a distinct concavity along its lateral outline (in dorsoventral view), such that at approximately one-third the distance anterior from the barbels to the tip of the snout the snout becomes significantly narrower (Fig. 3G-L). The elongate snout (i.e., preorbital length) is one of the most distinctive morphological features of *A. stellatus*, although there is notable variation in both the length and width of the snout, even between specimens from the same populations. However, compared to all other sturgeons, the snout of *A. stellatus* is much longer, and during ontogeny the snout (prebarbel length) grows substantially faster than other regions of the head (Fig. 4, line 1), particularly the orbital region, even at small sizes (<50 mm HL; Fig. 4). The postorbital length grows slightly slower than the snout region, but still faster than the orbital region (Fig. 4, line 2). This indicates that most of the elongation of the head is due to elongation of the snout.

Bones of the skull roof and circumorbital region (Figures 5-8)

The posterior portion of the skull roof of *Acipenser stellatus*, like that of other sturgeons (Hilton et al., 2011) is formed by a group of more or less stable elements (i.e., that are in similar position

and shape among individuals, although there may be some variation in precise shapes of elements). These elements are all heavily ornamented by ridges of bone radiating from the presumed center of ossification. These bones include the anteriormost dorsal scute, which becomes fully incorporated into the skull roof (i.e., articulates on three of its four sides with other bones of the skull roof). This scute is gently rounded posteriorly, and anteriorly bears a distinct, unornamented median process that is covered dorsally by the narrow, triangular median extrascapular. Laterally, the anteriormost dorsal scute overlaps the posttemporal, which forms the posterolateral corner of the skull roof. The ventral surface of the posttemporal has a large descending lamina of bone, which embraces the lateral surface of the occipital region of the neurocranium. The posttemporal is overlapped by a series of lateral extrascapulars, which vary in number (both between individuals and bilaterally). The lateralmost lateral extrascapular carries the confluence between the supratemporal, occipital, and trunk lateral-line sensory canals.

Anterior to the extrascapular series, are two paired elements, the dermopterotic laterally, and the parietal medially, that form a band across the entire posterior portion of the skull roof. The left and right parietals meet each other along most of their midline (though even in relatively large juveniles there may be a narrow gap between the elements; Fig. 6). The dermopterotics form much of the lateral margins of the skull roof posterior to the orbits, and carry the supratemporal lateral-line sensory canal. Anterior to both the parietals and the dermopterotics are the frontals. These bones are among the largest elements of the skull roof. The frontal receives the supraorbital lateral-line sensory canal from the dermosphenotic, and carries it anteriorly to the plate-like nasal, which is small in comparison to other sturgeons (Hilton et al., 2011), and then on to the tubular nasal.

Two elements form the dorsal margin of the orbit, the supraorbital anteriorly and the dermosphenotic posteriorly. The supraorbital has a prominent, posteriorly angled ventral process; this process, as in most sturgeons, is unornamented and does not contact any other elements. The dermosphenotic is intercalated between the supraorbital and the postorbital, which is a robust, irregularly rectangular bone; the postorbital forms the posterior margin of the orbit and carries the infraorbital sensory canal from the dermosphenotic ventrally to the jugal. For consistency with other recent studies of the osteology of sturgeons, we use the term jugal herein for this bone, although as shown by Rizzato et al., 2020, this bone is likely not homologous to the jugal of other osteichthyans. The jugal of *Acipenser stellatus* has a relatively small dorsal arm (relative

to taxa such as *A. oxyrinchus*; EJH pers. obsv.), and a much-elongated anterior arm. In ventral view, there is no distinct median process on the jugal of *A. stellatus* (Figs. 6, 7), which is similar to the condition found in *Pseudoscaphirhynchus* (Hilton, 2005). The anterior tip of the anterior arm of the jugal contacts the posteriormost border rostral bone. Medially, the jugal carries the infraorbital sensory canal into the series of rostral canal bones, which comprises irregularly numbered and shaped elements. The rostral canal bones follow the path of the rostral canal, which is the anterior extension of the infraorbital lateral line sensory canal. The rostral sensory canal bends medially just anterior to the level of the barbels before bending again to course anteriorly, parallel to the lateral margins of the ventral rostral bone series. The left and right series of rostral canal bones meet together at the rostral canal commissure. On either side of this commissure is a distinctly shaped, tripartite canal bone, the lateral rostral bone (Hilton, 2002), which is homologous to the antorbital of other basal actinopterygians (Warth et al., 2017; Rizzato et al., 2020).

Anamestic bones of the dorsal rostrum (Figures 5-8)

The anterior portion of the dermal skull roof (i.e., the snout) is armored by two distinct series of bones, the dorsal rostral bones and the border rostral bones. All elements of the snout are irregular in their shape, but the two series can be readily distinguished. The dorsal rostral bones, which lie dorsal and medial to the ampullary fenestrae, are generally elongate and narrow. This is in contrast to the border rostral bones, which are more rectangular in form.

Braincase (Figures 9, 10)

The basic form of the neurocranium of *Acipenser stellatus* is similar to that of other members of the genus (see Hilton et al., 2011: figs. 10, 29, and 41). The primary difference is that the neurocranium of *A. stellatus* is much narrower than that of other species, particularly anteriorly. It also has a distinctly concave profile in lateral view (Fig. 9B). No chondral ossifications were present in the braincase of our specimens. Although these included adult specimens, this absence may be related to ontogeny, as only the largest and presumably oldest specimens of *A. brevirostrum* examined by Hilton et al. (2011) were found to have ossifications associated with a largely cartilaginous neurocranium. The anteriormost region of the neurocranium is the rostroethmoid. Ventrally, the rostroethmoid region supports a broad patch of ventral rostral

bones medially, and a pair of deep grooves that run the length of the snout. Dorsally the rostroethmoid region is marked by longitudinal grooves; more posteriorly on the dorsal surface of the neurocranium, these grooves become more irregular and reticulate. The postnasal wall and lateral ethmoid process demarcate the rostroethmoid region and the orbital region. In dorsoventral view, the neurocranium has a distinct notch at this level, separating the postnasal wall anteriorly and the orbital shelf posterodorsally. The posterior portion of the neurocranium (comprising the orbital, otic, and occipital regions) is roughly hourglass shaped in dorsal view. The orbital region is the widest region, although the occipital region is almost as wide at the point it flares laterally supporting the posttemporal processes, which are wing-like and closely associated with the ventral flanges of the posttemporals. There are at least five vertebral segments fused to the posterior portion of the occipital region of the neurocranium (based on distinct neural arches that are continuous with the cartilage of the occipital region).

The shape of the parasphenoid of *Acipenser stellatus* is typical for acipenserids (Fig. 10), and is formed by a broad flat plate that is closely associated with the ventral surface of the otic region of the neurocranium. Posteriorly, this region of the parasphenoid is pierced by two foramina for the efferent branchial arteries, and is marked by a ridge of bone, which marks the region of contact with the dorsal gill arch elements. There are two anterodorsally directed ascending rami that define the boundary between the otic and orbital regions. Posteriorly, there are two greatly exaggerated posterior extensions, separated by a deep aortic notch. These posterior processes support the occipital region of the braincase, and extend posteriorly to support the anterior vertebrae (posterior to the margin of the skull roof). Extending anteriorly from the main body of the parasphenoid is a median anterior process, which ventrally forms a ridge of bone that is enveloped by the cartilage of median ventral ridge of the neurocranium (Fig. 10; not visible in Fig. 9C, as it is completely embedded in the cartilage of the neurocranium). Anteriorly, this median process of the parasphenoid contacts the posteriormost ventral rostral bone, which is single median element that continues the ridge-like form of the median anterior process. Anterior to this posterior ventral rostral bone is a series of smaller, flat, ventral rostral bones. Each of these elements is distinct in shape and size, although they are all elongate.

Opercular series (Figure 11)

As in all extant Acipenseridae, the only elements of the opercular series in *Acipenser stellatus* are the subopercle and two branchiostegals. The suboperecle is a large, plate like element with a scalloped posterior margin. As in most acipenserids, its anterior margin has a slight extension, but lacks the distinct anterior process found in some taxa, including *Scapirhynchus* and *Pseudoscaphirhynchus* (Findeis, 1997: fig. 7). The medial surface of the subopercle is mostly smooth, with some radiating grooves near the margin, indicating the scalloped region. Most of the lateral surface of the subopercle is heavily ornamented with ridges of bone. The anterior margin is smooth, where it is covered by a thick layer of dermis. Ventrally, the subopercle tightly overlaps the dorsolateral surface of the dorsal most branchiostegal, which is narrow dorsally, and flares out ventrally, where it contacts the more plate-like ventral branchiostegal. The ventral flared region of the dorsal branchiostegal, and the external surface of the ventral branchiostegal are ornamented by ridges of bone.

As is typical of extant Acipenseridae, *Acipenser stellatus* lacks a distinct preopercle. Rather, the dorsal portion of the preoperculomandibuilar canal is enclosed by a series of tubular bones that is positioned between the postorbital and jugal anteriorly and the subopercle and branchiostegals posteriorly, and is situated among a field of small, bony plates (Fig. 6B, C).

Palatoquadrate and its ossifications (Figure 12)

The upper jaw comprises a large cartilaginous element, the palatoquadrate, and its associated dermal bones (dermopalatine, ectopterygoid, palatopterygoid, and quadratojugal) and the chondral autopalatine bone, as well as the posterior cartilaginous palatal complex. Note that the element termed the dermopalatine is possibly homologous to the maxilla of other actinopterygians (Datovo and Rizzato, 2018), and the palatopterygoid likely represents the endopterygoid of other actinopterygians; for consistency with our other recent descriptions of the osteology of Acipenseridae (Grande and Hilton, 2006; Hilton et al., 2011, 2016), we use dermopalatine and palatopterygoid here with the acknowledgment that the other terms may be more accurate.

The dermopalatine lines the anterior margin of the palatoquadrate cartilage, is distinctively bent in its mid-portion, and has a moderately well-developed flange along its anterior margin. This condition is similar to other acipenserids, but the flange is not as large as that found in some taxa (e.g., *Acipenser baerii*, *Pseudoscaphirhynchus* spp.). The dermopalatine

contacts the ectopterygoid along its posterior margin at its midpoint, and the quadratojugal at its lateralmost point. The quadratojugal is broadest anteriorly at its point of contact with the dermopalatine but is relatively stout along its entire length. The ectopterygoid is also broadest anteriorly where it contacts the dermopalatine, but it tapers to a sharp point posteriorly where it contacts the palatopterygoid. The palatopterygoid is enveloped by cartilage on most of its dorsal surface, and has broad, pointed, and exposed bony arms that contact the ectopterygoid laterally and that approaches its antimere medially, where it contacts the ventral surface of the autopalatine (Fig. 12C). The *pars quadrati* of the palatoquadrate, lateral to the palatopterygoid, is unossified and forms a cartilage-to-cartilage jaw joint with Meckel's cartilage. The median portion of the palatoquadrate – the *pars palatini* – contacts its antimere along the midline and is formed by a large, flat sheet of cartilage. At the center, of this cartilage is a well-ossified, circular autopalatine.

The palatal complex, which is a structure unique to Acipenseridae (Hilton et al., 2011), is rounded posteriorly in *Acipenser stellatus*, and is formed by a series of irregularly shaped and sized cartilages. The central cartilage is largest, but is not as large as that found in other taxa (e.g., *Huso*). The anterior margin of the palatal complex extends anteriorly, and separates the median arms of the left and right palatopterygoid from one another. Lateral to this median point, the anterior margin of the palatal complex is smoothly concave.

Lower jaw (Figure 13)

As in all acipenserids, Meckel's cartilage of *Acipenser stellatus* is the dominant element of the lower jaw, and extends the entire length of the jaw. The posterior portion of Meckel's cartilage is the most robust portion of the element, and bears a deep, broad articulatory surface for contact with the palatoquadrate; there is no indication of an ossified articular. The dentary is the largest bone found in the lower jaw, and is roughly uniform in its width for its entire length, though it does taper to a rounded point on both its anterior and posterior ends. The dentary is edentulous in our specimens, but this is due to the advanced ontogenetic stages examined. The dentary forms a slight shelf anteriorly, but it is not as exaggerated as in some sturgeons, such as *A. baerii*. The dermal prearticular forms along the posteromedial portion of Meckel's cartilage, and defines the anterior point of the insertion of the jaw adductor musculature. The only other ossification of the

lower jaw is the mentomeckelian, which is a small, rectangular collar of bone positioned near the anterior tip of Meckel's cartilage.

Hyoid arch (Figures 14, 15)

The largest element of the hyoid arch in *Acipenser stellatus* is the hyomandibula (Fig. 14). The dorsal articulatory head, which articulates with the neurocranium just posterior to the dorsal tip of the ascending process of the parasphenoid, is rounded and circular in cross section. The ossified portion of the hyomandibula is largely confined to the dorsal portion of the hyomandibular cartilage. In our large specimens of *A. stellatus*, we found cartilage on the external surface of the hyomandibula (termed the external hyomandibular cartilage, by Hilton et al., 2011 for *A. brevirostrum*); similar cartilage was found on the anterior ceratohyal (below). The hyomandibula is narrowest dorsally, and flared posteroventrally where it follows the outline of the hyomandibular cartilage. The hyomandibular cartilage has a large exposed portion posteroventrally that forms the ventral hyomandibular blade, which is drawn out to a ventral point that articulates with the interhyal (Fig. 14). In our adult specimens of *A. stellatus*, the interhyal of is entirely cartilaginous (i.e., lacks the ossification found in taxa such as *A. brevirostrum*; Hilton et al., 2011).

The ventral portion of the hyoid arch comprises a small, cartilaginous posterior certatohyal cartilage, a large ossified anterior ceratohyal, and a cartilaginous hypohyal (Fig. 15). The anterior certatohyal is roughly hour-glass shaped, with a deeper dorsal concavity and a shallow ventral concavity. Within the dorsal concavity, we found an external hyoid arch cartilage on the surface of the bone, as on the hyomandibula (Fig. 14). The hypohyal is a small, somewhat pyramidal cartilage that contacts the anterior ceratohyal laterally, the hypobranchial 1 posteriorly, and the basibranchial copula medially (Fig. 15). The anterior face of the hypohyal is slightly concave.

Gill arches (Figures 15-17)

The ventral portion of the gill arches comprise two median basibranchial copulae, and paired hypobranchials (1-3) and certatobranchials (1-5). The anterior basibranchial copula is large, broad, and supports the hypohyal and all three of the hypobranchials. Posteriorly, there is a small posterior basibranchial copula that does not contact any other branchial elements except the

anterior basibranchial copula. In our large, hand-cleaned skeletal specimens, we were unable to find a thin median cartilage posterior to the basibranchial copula (i.e., the unnamed cartilage illustrated by Hilton et al. 2011 for *A. brevirostrum*), but it may have been removed during preparation. However, it was confirmed to be absent in our smaller cleared-and-stained specimens (e.g., UMMZ 184980, 112 mm SL). There are three cartilaginous hypobranchials present in our specimens of *A. stellatus*, although in other species of *Acipenser* there is a fourth hypobranchial variably present (intraspecifically, and bilaterally). Hypobranchial 1 is the largest, and bears an anterior process that forms a thin, rounded shelf dorsal to the hypohyal. A medial process contacts the anterior end of the anterior basibranchial copula. Hypobranchials two and three are sequentially smaller. Hypobranchial 3 is unique within the series in bearing a ventral process that curves and meets its antimere, forming a canal ventral to the basibranchial copula (Fig. 15B); this is present in other species of *Acipenser* as well. All certatobranchials bear a groove on their ventral surfaces to house the branchial blood vessels. Certatobranchials 1-3 are similar in shape to one another, but become sequentially smaller more posteriorly. Certaobranchials 4 and 5 are proximally flattened, with the cartilaginous tip of certaobranchial 4 twisting slightly to form a channel. This is unlike the proximal tips of ceratobranchials 1-3, which are blunt where they contact the hypbranchials.

The dorsal portion of the gill arches (Fig. 16) comprise four epibranchials (1-4), three infrapharyngobranchials (1-3), and two suprapharyngobranchials (1-2). Of these, only the epibranchials 1 and 2 were found to be ossified in our specimens, with the other elements remaining cartilaginous. Epibranchial 1 is the largest of the series and has a distinct dorsal groove, which houses the branchial blood vessels. Epibranchial 4 is unique among the series in being grooved distally, but flattened and spatulate proximally. The infrapharyngobranchials articulate with the proximal tips of the epibranchials, and are blunt to rounded proximally. The suprapharyngobranchials articulate with dorsally directed cartilaginous processes of the epibranchials 1 and 2.

The gill rakers of *Acipenser stellatus* are found on the leading and trailing edges of all arches, and are supported by the hypohyals, ceratobranchials, and epibranchials. Those of the leading edge of the first arch are narrow and pointed (Fig. 17). Those of the trailing edge of the first arch and the more posterior gill arches are generally shorter, wider, and have rounded tips.

They are irregularly shaped, however, and may be bifurcated, particularly on the trailing edges of the arches (Fig. 17).

Discussion

This study provides a description of the skull of *Acipenser stellatus*, and is intended to complement data that is available for other species of sturgeons. We use these new morphological data to discuss two aspects of the skull of sturgeons generally, with particular reference to *A. stellatus*. First, we discuss the course of the sensory canals in the posterior region of the skull roof of sturgeons. Second, we discuss the presence and morphology of spines on the dermal bones of the skull roof, and clarify their distribution among sturgeons.

Sensory canals of the occipital region (Figures 8, 18)

The branching pattern between the trunk lateral-line sensory canal, the occipital sensory canal, and the supratemporal sensory canal was first used as a character in a phylogenetic analysis of Acipenseridae by Findeis (1997: character 56). He found the conjunction of these canals within the lateral extrascapular to be a synapomorphy of *Pseudoscaphirhynchus* (note that these canals correspond to the postotic [= supratemporal] and supratemporal [= occipital and trunk lateral line] of Rizzato et al. 2020, but we are using the terminology used by Findeis and others for Acipenseriformes). Indeed, *Scaphirhynchus*, *Huso*, and most *Acipenser* species have this branching in the posttemporal, whereas *Pseudoscaphirhynchus* has it in the lateral extrascapular as described by Findeis (1997; Fig. 18). Hilton (2005) first noted that a similar condition to that in *Pseudoscaphirhynchus* was found in juvenile specimens of *A. stellatus* available to him. This character was used as supporting morphological evidence for the sister group relationship between *A. stellatus* and *Pseudoscaphirhynchus* recovered by Birstein et al. (2002) based on genetic data. Herein we confirm this condition in adult specimens of *A. stellatus*. The conjunction of these canals within the lateral extrascapular was used by Hilton et al. (2011) as a character in their analysis and was found to have a much broader distribution within Acipenseriformes, and was found in †peipiaosteids, †chondrosteids, fossil polyodontids, †*Priscosturion*, and in non-acipenseriform actinopterygians (Grande and Hilton, 2006; Hilton and Forey, 2009; Hilton et al., 2011). It should be noted that Hilton et al. (2011) mistakenly cited this character (character 14, p. 127) as the confluence of the trunk, occipital, and supraorbital

canals, rather than the trunk, occipital, and supratemporal canals; this mistake was also made in Hilton and Forey (2009). Because of the broad distribution of this character, it is plesiomorphic for Acipsenseridae. Hilton et al. (2011) found the confluence of the trunk, occipital, and supratemporal sensory canals in the posttemporal to be homoplastic within the family, but further study of this character is required to better understand its distribution in Acipenseridae.

Intraspecific variation compounds the difficulty for the interpretation of this character. Hilton et al. (2016) found the confluence of the canals to be variable in a small sample of *A. sinensis*: some individuals had it housed in the lateral extrascapular; but in most specimens it was found in the posttemporal. Here we found a single specimen of *H. huso* to have this confluence in the lateral extrascapular on one side of the head; this element is positioned close to the lateral margin of the skull, in a position typically occupied by the posttemporal (Fig. 18C; left side). Further study of large series of specimens is necessary to determine the precise taxonomic distribution of this character.

Cranial spines (Figures 5, 19-21)

The exposed dermal bones of Acipenseridae, including the scutes, elements of the shoulder girdle, and the skull roof, generally are heavily ornamented with bony ridges forming various patterns. This ornamentation ontogenetically develops from small denticle-like structures that fuse together across ontogeny; the sharp points of the denticle-like structures become rounded and indistinct within the overall ornamentation (e.g., see Hilton et al., 2011). In some species, however, many of the dermal bones, including both the scutes and those of the head, may bear a distinctly raised ridge of bone that is produced into a thorn-like process or spine.

Findeis (1997) was the first to formalize morphological characters for use in a genus-level phylogenetic analysis of the family Acipenseridae. Among the characters he defined was the presence of cranial spines or spikes (his characters 41 and 55, respectively). The posttemporal and supracleithrum are included in this discussion of "cranial" spines because they are tightly associated with the skull, and the spines of these elements appear to be serially related to those of the skull roof proper. Findeis (1997) recovered the presence of spines in the center of the parietal, posttemporal, supracleithrum, and anterior dorsal rostral bones to be a synapomorphy of *Scaphirhynchus* + *Pseudoscaphirhynchus*. Hilton et al. (2011: character 13) only included the first of these characters (cranial spines) in their analysis. In addition to these

two genera, they also coded *Acipenser stellatus* as having spines on the dermal skull bones. This character was recovered as homoplastic, supporting both *Scaphirhynchus* spp. and *A. stellatus* + *Pseudoscaphirhynchus*. These authors also noted the difference in the gross morphology of the spines between the two groups (see below). Spines are clearly present on the skull bones of *A. stellatus*, and these persist into the adult stage, as confirmed here (Fig. 5C, D). However, the variation of cranial spines among sturgeon species is worthy of further consideration.

As noted by Hilton et al. (2011), Findeis' (1997) character of spikes present on the frontals (character 55) was a subjective distinction between the cranial spines of his character 41. Findeis (1997) acknowledged that "spikes" on the frontals, considered to be a synapomorphy of *Pseudoscaphirhynchus*, were only found in *P. kaufmanni*, which he considered to be representative of the genus. He further noted that *P. hermanni* "occasionally has weak spines on anterior dorsal rostral bones" (p. 111). Indeed, the thorn-like spines on *P. kaufmanni* are exaggerated compared to all other sturgeons. They are scattered on the anterior dorsal rostral bones, frontals, parietals, as well as the jugal, posttemporal, and supracleithrum (Fig. 19A). Spines may be present on the dermopterotic as well, although these are frequently asymmetrically present. Mayden and Kuhajda (1996) recorded spines present on both the frontal and parietal in *P. hermanni*. Kuhajda (2002) distinguished between straight and recurved spines on the skull of *Pseudoscaphirhynchus*, and noted variation in presence of spines that correlated to the various forms of the taxa (i.e., long-snout vs. short snout *P. hermanni* had no or a few spines at the tip of the snout, respectively). Most specimens of *P. fedtschenkoi* and *P. hermanni* (Fig. 19D-F) bear spines only on the posttemporal and supracleithrum, although in *P. hermanni* we did variably observe well-developed spines on the dorsal rostral bones and parietals and occasionally on the frontals (though the frontal more often has just strong ridge) (Fig. 19C, D). When spines are present in *P. fedtschenkoi* and *P. hermanni*, they are much smaller and less distinct from the typical ridge ornamentation of the skull bones. The spines of *P. hermanni* may be larger than those of specimens identified as *P. hermanni* x *P. kaufmanni* hybrids (Fig. 19B). Therefore, Findeis' (1997) assertion that the "presence of frontal spikes is distinctive of *Pseudoscaphirhynchus*" is overstated, since 1) enlarged spines on any dermal bones are only found in *P. kaufmanni*, and 2) when spines are present in *P. fedtschenkoi* and *P. hermanni* (intraspecifically variable in both), they are only rarely found on the frontals (and then only in *P. hermanni*).

519 Outside of the *Acipenser stellatus* + *Pseudoscaphirhynchus* clade, cranial spines are
520 found in several taxa, and these are of various size and extent (Fig. 20A-H). These spines may be
521 found on the anamestic dorsal rostral bones, as well as on some of the more stable bones (e.g.,
522 frontal, parietal, dermopterotic, and posttemporal). In many taxa, these spines disappear in adult
523 stages, although even this is variable both within and between species. For example, in relatively
524 small specimens of *Huso huso* and *H. dauricus,* there are spines on at least some skull bones. In
525 *H. huso*, spines were found on the supracleithrum, posttemporal, dermopterotic, dermosphenotic,
526 supraorbital, parietal, and frontal in several specimens ranging from 163 to 334 mm SL (ZIN
527 7207, ZIN 12177, ZIN 10626, ZMMU P-9119), but only on the supracleithrum, posttemporal,
528 parietal and frontal in other specimens (ZMMU 8189, n = 2, 142-187 mm SL). A spine was only
529 found on the supracleithrum and the posttemporal on a 138 mm SL specimen (ZMMU P12388),
530 whereas in a larger specimen (VIMS 34978; 1185 mm SL) all bones of the skull roof and
531 shoulder girdle are devoid of any spines. In *H. dauricus,* spines were only observed on the
532 supracleithrum and posttemporal, and occasionally on the parietal and the dermopterotic,
533 although these latter spines were weakly formed (Fig. 20A; 279-374 mm SL; ZMMU P-6103,
534 ZIN 12549, ZIN 3194, ZIN 3195).
535 In many species of *Acipenser*, relatively small specimens may have occasional spines
536 developed on some bones of the shoulder girdle and skull roof. For example, in *A. sturio*, spines
537 were found on the supracleithrum (ZMMU P-626, 268 mm SL; ZMMU P-13015, 318 mm SL),
538 whereas larger specimens (e.g., MNHN 1962-1295, 545 mm SL) were found to be completely
539 devoid of spines all together (Fig. 20B). Similarly, in *A. transmontanus*, spines were recorded on
540 the dorsal rostral bones of a small specimen (CAS uncat., acc 1952-VII:5A, 85.1mm SL), but
541 larger specimens have flattened bones. In cases where ontogenetic disappearance or reduction of
542 the spines occurs, the spines present in even small specimens are small and frequently restricted
543 to the supracleithrum, posttemporal, and sometimes the dermopterotic, frontal, and parietal. In *A.*
544 *gueldenstaedti* (e.g., ZMMU P-8191, 140-250 mm SL; ZMMU P-630, 289 mm SL; ZMMU P-
545 1462, c. 300 mm SL), *A. persicus* (e.g., ZMMU 20924, 175 mm SL; ZMMU P-20916, 149 mm
546 SL; ZMMU P-20291, 63-68 mm SL; ZIN 46978, 198 mm SL ZIN 46979, 133-165 mm SL), and
547 *A. colchicus* (e.g., ZIN 47444, 264 mm SL, ZMMU P-17606, 187-227 mm SL; MNHN 1925-54,
548 207 mm SL; MNHN 1970-72, 218 mm SL), small individuals can be extremely spinous, and
549 have these spines distributed on all skull roofing bones, including the dorsal rostral bones (Fig.

20G, H). Larger specimens may bear ridges or raised portions of these bones that are suggestive of where the spines were positioned at earlier stages, as noted by Findeis (1997; Fig. 20B-F). The presence of spines may also be individually variable, and not necessarily associated with ontogeny. For instance, spines occur rarely in *A. fulvescens* (e.g., only observed herein in MCZ 8911, 259 mm SL, on scl), whereas other specimens – both smaller and larger – are entirely devoid of spines. Specimens of other species of *Acipenser* that we observed to possess small (but distinct) cranial spines include *A. baerii* (ZMMU P-3312, 273-303 mm SL on scl and pa; ZIN 13596, 374-440 mm SL on pt, scl, fr/dpt; ZIN 10641, 272-338 mm SL, on scl, pt, dpt, fr, pa, dsp, so, excm; ZIN 10888, 271 mm SL, on fr, pa, scl, pt, dsp), *A. medirostris* (CAS uncat. acc. 1952-X:4, 635 mm SL), *A. mikadoi (*ZMMU P20290, 44 mm SL, on scl, pt; ZIN 50527, 239 mm SL, on scl), *A. nudiventris* (ZMMU P3331, 193 mm SL, on scl, pt, dpt; ZIN 4509, 210-224 mm SL, on scl, pt, dpt; ZIN 4508, 352 mm SL, on scl, pt), and *A. schrenki* (ZMMU P-9348, 324-378 mm SL, on scl; ZMMU 7708, 450 mm SL, on scl, pt; ZIN 17934, 206-313 mm SL, on scl, pt). None of these taxa ever were found to have spines on their dorsal rostral bones. Spines were not recorded for any specimens of *A. brevirostrum* (n=198, 9.5-930 mm SL), *A. naccari* (n=9, 162-562 mm SL), *A. oxyrinchus* (n=13, 480-1700 mm SL), or *A. ruthenus* (n=17, 178-464 mm SL),

The spines found in species of *Acipenser* and *Pseudoscaphirhynchus* differ in morphology from those found in *Scaphirhynchus*, which are much smaller, more flattened and posteriorly directed (Fig. 21); these are described as being "retrorse" (Berg, 1948; Bailey and Cross, 1954; Mayden and Kuhajda, 1996) and differ from the hooked or thorn-shaped spines discussed above. Within *Scaphirhynchus*, there is significant variation among the three species (Mayden and Kuhajda, 1996). Although determining the exact taxonomic distribution of spines on the skull bones of sturgeons is beyond the scope of this study, it is clear that they are more widespread and may carry phylogenetic signal. Ontogenetic variation of cranial spines in sturgeons is particularly difficult to study, and clarification will only come from studies of large series of specimens representing the entire ontogeny of a single species.

Acknowledgements

We thank the following curators and collections staff for their hospitality during museum visits and for access to specimens: Ekaterina Vasil'eva (ZMMU), Arkady Balushkin and Boris Sheiko (ZIN), Patrice Pruvost (MHNH), Bernie Kuhajda (UAIC), Dave Catania (CAS), Doug Nelson

(UMMZ), Karsten Hartel and Andrew Williston (MCZ); Sarah Huber (VIMS) provided curatorial assistance. This research was supported in part by the U.S. National Science Foundation (DEB-0841691, to EJH and CBD). Drafting of this manuscript benefited from the support of the Winter 2020 William & Mary Faculty Writers' Retreat, sponsored by the Provost's Office and William & Mary Libraries. This is contribution number 3927 of the Virginia Institute of Marine Science, William & Mary.

References

Antipa, G. 1909. Fauna Ichtiologică a României (Ichthyological Fauna of Romania). *Academia Română - Publicaţiunile Fondului Vasile Adamachi* **16:** 239-273.

Antoniu Murgoci, A. 1937a. Particularités anatomiques qui différencient le genre *Huso* du genre *Acipenser* dans les eaux roumaine (Danube et Mère Noire). *Annales Scientifiques de l'Université de Jassy* **23:** 94-103.

Antoniu Murgoci, A. 1937b. Note sur les espèces du genre *Acipenser* L. *Annales Scientifiques de l'Université de Jassy* **23:** 104-108.

Atoniu-Murgoci, A. 1942. Contributions a l'étude des Acipenseridés de Roumanie. *Annales Scientifiques de l'Université de Jassy* **28:** 289-385.

Bailey, R. M. and Cross, F. B. 1954. River sturgeons of the American genus *Scaphirhynchus*: characters, distribution and synonymy. *Papers of the Michigan Academy of Science, Arts, and Letters* 39:169-208.

Bakhshalizadeh, S., Bani, A. and Abdolmalaki, S. 2013. Comparative morphology of the pectoral fin spine of the Persian sturgeon *Acipenser persicus*, the Russian sturgeon *Acipenser gueldenstaedtii*, and the Starry sturgeon *Acipenser stellatus* in Iranian waters of the Caspian Sea. *Acta Zoologica (Stockholm)* 94: 471–477.

Bemis, W. E., Hilton, E. J., Brown, B., Arrindell, R., Richmond, A. M., Little, C., Grande, L., Forey, P. L., and Nelson, G. J. 2004. Methods for preparing dry, partially articulated skeletons of osteichthyans, with notes on making Ridewood dissections. *Copeia* **2004:** 603–609.

Bemis, W. E., Findeis, E. K., and Grande, L. 1997. An overview of Acipenseriformes. *Environmental Biology of Fishes* **48:** 25-72.

Berg, L. S. 1948. The Freshwater Fishes of the USSR and Adjacent Countries. 4th Edition, Part 1. Akademia Nauk USSR, Moscow. [in Russian; English translation published by Israel Program for Scientific Translations, Jerusalem, 1965].

Birstein, V. J. and Vasil'ev, V. P. 1987. Tetraploid–octoploid relationships and karyological evolution in the order Acipenseriformes (Pisces): karyotypes, nucleoli, and nucleolus-organizer regions in four acipenserid species. Genetica **73:** 3–12.

Birstein, V. J., Doukakis, P., and DeSalle, R. 2002. Molecular phylogeny of Acipenseridae: Nonmonophyly of Scaphirhynchinae. *Copeia* **2002:** 287-301.

Borzenko, M. P. 1942. Kaspiĭskaya sevryuga (sistematicka, biologiya i promȳsel). *Izvestiya Azerbaĭdzhanskoĭ nauchno-issledovatel'skoĭ rȳbokhozyaĭstvennoĭ stantsii* **7:** 3-114. [not seen]

Chicca M., Suciu, R., Ene, C., Lanfredi, M., Congiu, L., Leis, M., Tagliavini, J., Rossi, R., Fontana, F. 2002. Karyotype characterization of the stellate sturgeon, *Acipenser stellatus*, by chromosome banding and fluorescent in situ hybridization. *Journal of Applied Ichthyology* **18:** 298 – 300.

Datovo, A., and Rizzato, P.P., 2018, Evolution of the facial musculature in basal ray-finned fishes: *Frontiers in Zoology* **15**: 1-29.

Dillman, C. B., and Hilton, E. J. 2015. Anatomy and development of the pectoral girdle, fin, and fin spine of sturgeons (Actinopterygii: Acipenseridae). *Journal of Morphology* 276: 241-260.

Dillman, C. B., Wood, R. M., Kuhajda, B.R., Ray, J.M., Salnikov, V.B., and Mayden, R. L. 2007. Molecular Systematics of the Shovelnose Sturgeons (Scaphirhynchinae) of North America and Central Asia. *Journal of Applied Ichthyology* **23:** 290-296.

Dingerkus, G., and Uhler L. D. 1977. Enzyme clearing of alcian blue stained whole small vertebrates for demonstration of cartilage. *Journal of Stain Technology* **52:** 229-232.

Findeis, E. K. 1997. Osteology and phylogenetic relationships of recent sturgeons. *Environmental Biology of Fishes* **48:** 73-126.

Fitzinger, L.J. and Heckel, J. 1836. Monographische Darstellung der Gattung *Acipenser*. Annalen des Wiener Museums der Naturgeschichte. **1:** 261-326.

Fontana, F. 2002. A cytogenetic approach to the study of taxonomy and evolution in sturgeons. *Journal of Applied Ichthyology* **18:** 226-233.

Fricke, R., Eschmeyer, W. N. and Van der Laan, R., eds. 2020. Eschmeyer's Catalog of Fishes: Genera, Species, References. (http://researcharchive.calacademy.org/research/ichthyology/catalog/fishcatmain.asp). Electronic version accessed 02 Sep 2020.

Friedrich, T. 2018. Danube sturgeons: past and future. In: Schmutz S. and Sendzimir J. (Eds): Riverine Ecosystem Management, Aquatic Ecology Series 8, pp. 507-518. Springer, Cham. https://doi.org/10.1007/978-3-319-73250-3_26

Grande, L., and Hilton, E. J. 2006. An exquisitely preserved skeleton representing a primitive sturgeon from the Upper Cretaceous Judith River Formation of Montana (Acipenseriformes: Acipenseridae: n. gen. and sp.). *Journal of Paleontology, Memoir* ***65*****:** 1-39.

Grande, L., and Hilton, E. J. 2009. A replacement name for †*Psammorhynchus* Grande & Hilton 2006 (Actinopterygii, Acipenseriformes, Acipenseridae). *Journal of Paleontology* **83:** 317-318.

Heckel J., and Kner, R. 1858. Die Süßwasserfische der östreichischen Monarchie. W. Engelmann, Leipzig.

Hilton, E. J. 2005. Observations on the skulls of sturgeons (Acipenseridae): shared similarities of *Pseudoscaphirhynchus kaufmanni* and juvenile specimens of *Acipenser stellatus.* *Environmental Biology of Fishes* **72:** 135–144.

Hilton, E. J., and Bemis, W. E.. 2012. External morphology of shortnose sturgeon, *Acipenser brevirostrum* (Acipenseriformes: Acipenseridae), from the Connecticut River, with notes on variation as a natural phenomenon. In: Kynard, B., Bronzi, P., and Rosenthal, H. (Eds). Life History and Behaviour of Connecticut River Shortnose and Other Sturgeons. pp. 243-265. Special Publication 4, World Society of Sturgeon Conservation.

Hilton, E. J. and Forey, P. L. 2009. Redescription of †*Chondrosteus acipenseroides* Egerton, 1858 (Acipenseriformes, Chondrosteidae) from the Lower Lias of Lyme Regis (Dorset, England), with comments on the early evolution of sturgeons and paddlefishes. *Journal of Systematic Palaeontology* **7:** 427-453.

Hilton, E. J., and Grande, L. 2006. Review of the fossil record of sturgeons, family Acipenseridae (Actinopterygii: Acipenseriformes), from North America. *Journal of Paleontology* **80:** 672-683.

673 Hilton, E. J., Grande, L., and Bemis, W. E.. 2011. Skeletal anatomy of the shortnose sturgeon,
674 *Acipenser brevirostrum* Lesueur 1818, and the systematics of sturgeons
675 (Acipenseriformes, Acipenseridae). *Fieldiana (Life and Earth Sciences)* **3:** 1-168.
676 Hilton, E.J., Dillman, C.B., Zhang, T., Zhang, L., and Zhuang, P. 2016. The skull of the Chinese
677 sturgeon, *Acipenser sinensis* (Acipenseridae). *Acta Zoologica (Stockholm)* **97:** 419-432.
678 Holčík, J. 1959**.** Nález jesetera hviezdnatého (*Acipenser stellatis* Pallas, 1771) v Dunaji pri
679 Komárne. *Zborník Slovenského Národného Múzea / Prírodné vedy* **5**: 39-43. [not seen]
680 Holostenco, D., Onără, D.F., Suciu, R., Honţ, Ş., and Paraschiv, M. 2013. Distribution and
681 genetic diversity of sturgeons feeding in the marine area of the Danube Delta Biosphere
682 Reserve. *Scientific Annals of the Danube Delta Institute* **19:** 25-34 doi:
683 10.7427/DDI.19.04.
684 Honţ, S., Paraschiv, M., Iani, M.I., Taflan, E., Holostenco, D.N., Oprea, D., and Oprea L. 2019.
685 Detailed analysis of beluga sturgeon (*Huso huso*) and stellate sturgeon (*Acipenser*
686 *stellatus*) migration in the Lower Danube River. *Turkish Journal of Zoology* **43:** 457-464.
687 doi:10.3906/zoo-1902-32.
688 Kittary, M. 1850. Recherches anatomique sur les poissons du genre *Acipenser*. *Bulletin de la*
689 *Société Impériale Naturalistes de Moscou* **23:** 389-445.
690 Kolvachuk, O.M., and Hilton, E.J. 2017. Neogene sturgeon (Acipenseriformes, Acipenseridae)
691 remains from southeastern Europe. *Journal of Vertebrate Paleontology* **e1362644** (7
692 pages).
693 Kovalev, K.V., Balashov, D.A., Cherniak, A.L., Lebedeva, E.B., Valsil'eva, E.D., and Vasil'ev,
694 V.P. 2014. The karyotype of the Amu Darya Sturgeon, *Pseudoscaphirhynchus kaufmanni*
695 (Actinopterygii; Acipenseridae). *Acta Ichthyologica et Piscatoria* **44:** 111-116.
696 Krieger, J., Hett, A.K. Fuerst, P.A., Artyukhin, E., and Ludwig, A. 2008. The molecular
697 phylogeny of the order Acipenseriformes revisited. *Journal of Applied Ichthyology,* **24,**
698 **supplement 1:** 36-45
699 Kynard, B., Suciu, R., and Horgan, M. 2002. Migration and habitats of diadromous Danube
700 River sturgeons in Romania: 1998-2000. *Journal of Applied Ichthyology* **18:** 529-535.
701 Kuhajda, B. R. 2002. Systematics, taxonomy, and conservation status of sturgeon in the
702 subfamily Scaphirhynchinae (Actinopterygii, Acipenseridae). Ph.D. Dissertation,
703 University of Alabama, Tuscaloosa, USA.

Lëvin, A. V., Bezrukanikov, A. P., and Pirogovskiĭ, M I. 1981. Osobennosti vertikal'nogo raspredeleniya osetrovȳkh v Severnom Kaspii. In: Ratsional'nȳe osnovȳ vedeniya osetrovogo khozyaĭstva, pp. 143-144. Tezisȳ dokladov nauchno-prakticheskoĭ konferentsii. Volograd. [not seen]

Mayden, R. L. and Kuhajda, B. R. 1996. Systematics, taxonomy, and conservation status of the endangered Alabama sturgeon, *Scaphirhynchus suttkusi* Williams and Clemmer (Actinopterygii, Acipenseridae). *Copeia* **1996:** 241-273.

Naderi, M., Asgharzadeh, A., Majid Haji Moradlo, A., and Ghorbani, R. 2016. Food Habits of Stellate Sturgeon, *Acipenser stellatus* Pallas, 1771, in South-Eastern Parts of the Caspian Sea, Iran. *Acta Zoologica Bulgarica* **68:** 395-398.

Nowruzfashkhami, M. R. and Khosroshahi, M. 1999. Karyotype study on stellate and great sturgeon by leukocyte culture. *Journal of Applied Ichthyology* **15**: 283.

Pallas, P. S. 1771. Reise durch verschiedene Provinzen des russ ischen Reiches. Gedruckt bey der Kayserlichen academie der wissenschaften. St. Petersburg.

Rizzato, P.P., Pospíšilova, A., Hilton, E.J., Bockmann, F.A. 2020. Development and homology of bones associated with lateral-line canals in the Senegal Bichir, *Polypterus senegalus* (Cladistii: Polypteriformes), with a discussion about the interrelationships between lateral-line canals and bone formation in the skull of fishes. *Journal of Anatomy.* **in press:** 1-29. https://doi.org/10.1111/joa.13202

Ruban G, Khodorevskaya, R., and Shatunovskii, M. 2019. Factors influencing the natural reproduction decline in the beluga (*Huso* , Linnaeus, 1758), Russian sturgeon (*Acipenser gueldenstaedtii,* Brandt & Ratzeburg, 1833), and stellate sturgeon (*A. stellatus*, Pallas, 1771) of the Volga–Caspian basin: A review. *Journal of Applied Ichthyology* **35:** 387-395.

Sabaj, M.H. 2019. Standard symbolic codes for institutional resource collections in herpetology and ichthyology: An Online Reference. Version 7.1 (21 March 2019). American Society of Ichthyologists and Herpetologists, Washington, DC. Available at: http://www.asih.org.

Sato, H., Murray A.M., Vernygora, O. and Currie, P.J. (2018). A rare, articulated sturgeon (Chondrostei: Acipenseriformes) from the Upper Cretaceous of Dinosaur Provincial Park, Alberta, Canada. Journal of Vertebrate Paleontology. 38: 1-15, DOI: 10.1080/02724634.2018.1488137.

735 Shubina, T.N., Popova, A.A., and Vasil'ev, V.P. 1989. *Acipenser stellatus* Pallas, 1771. In:
736 Holcik, J. (Ed). The Freshwater Fishes of Europe, vol. 1, part. 2. General introduction to
737 fishes. Acipenseriformes, pp. 395-444. AULA-Verlag, Wiesbaden.
738 Suciu, R., and Ene, C. 1996. Karyological study of the stellate sturgeon, *Acipenser stellatus*,
739 from the Danube River. *The Sturgeon Quarterly* 4: 14-15.
740 Suciu, R., and Guti, G. 2012. Have sturgeons a future in the Danube River? *Limnological*
741 *Reports* **39:** 19-30.
742 Vecsei, P., Suciu, R., Peterson, D., and Artyukhin, E. 2007. Threatened fishes of the world,
743 *Acipenser stellatus*, Pallas, 1771 (Acipenseridae). *Environmental Biology of Fishes* **78:**
744 211–212.
745 Vecsei, P., Charette, R., Trukshin, I., Maliepaard, T., Hochleithner, M., and Lafleur, Y. 2001.
746 CITES Identification Guide - Sturgeons and Paddlefish. Environment Canada, Ottawa.
747 Warth, P., E.J. Hilton, B. Neumann, L. Olsson & P. Konstantinidis. 2018. Development of the
748 muscles associated with the mandibular and hyoid arches in the Siberian sturgeon,
749 *Acipenser baerii*. *Journal of Morphology* 279: 163–175.
750 Warth, P., Konstantinidis, P., Naumann, B., Olsson, L., and Hilton, E.J. 2017. Description and
751 comparison of cranial development of Siberian sturgeon (*Acipenser baerii*) and Russian
752 sturgeon (*Acipenser gueldenstaedtii*). *Journal of Morphology* **278:** 418-442.
753 **Figure captions**
754
755 **Figure 1.** *Acipenser stellatus*. A, whole individual in lateral view. Head in B, ventral, and C,
756 dorsal views. D, 1400 mm TL specimen from the Volga River (Caspian Sea stock, long rostrum
757 form). E, 1550 mm TL specimen from the Kuban River (Sea of Azov stock; short rostrum form).
758 Illustrations in A-C from Fitzinger and Heckel (1836: plate 26, fig. 6 and plate 30, figs. 14 and
759 13, respectively). Illustrations in D and E by Dr. Paul Vecsei and used with permission. Anterior
760 facing left (A reversed from original).
761
762 **Figure 2.** Measurements taken on specimens of *Acipenser stellatus*.
763
764 **Figure 3.** Heads of *Acipenser stellatus*, in A, D, G, J, dorsal, B, E, H, K, lateral, and C, F, I, L,
765 ventral views showing variation in head shapes across a range of sizes. A, B, C (VIMS 42686,

27.5 mm TL). D, E, F, VIMS 42689 (37.5 mm TL); G, H, I, UMMZ 148980, 160 mm SL. J, K, L, from ZIN 15027, 455 mm SL. Anterior facing left; scale bar equals 1 mm (A-F), 10 mm (G-I), or 20 mm (J-L).

Figure 4. A, Growth trajectory of the head in a sample of *Acipenser stellatus* (y = 0.28x +7.88; n= 38). B, Comparison of growth trajectories of three portions of the snout length in a sample of *A. stellatus*: variable 1 = prebarbel length (y = 0.47x -1.88; n= 40); variable 2 = prenares length minus prebarbel length (y = 0.09x + 0.17; n= 40); variable 3 = preorbital length minus prenares length (y = 0.06x + 1.22; n= 40); variable 4 = head length minus preorbital length (y = 0.38 + 0.48; n= 40).

Figure 5. Skull of *Acipenser stellatus*. A, dorsal view of skull roof, and B, stable bones of the posterior portions of the skull roof. From Kittary (1850: plate 7, figs. 5 and 6). C, cleared and stained specimen in lateral view (UMMZ 148980, 160 mm SL). D, dry skeleton in lateral view; opercular series, jaws, and gill arches removed (VIMS 13552, 235 mm HL). Anterior facing left; scale bar equals 10 mm (C) or 20 mm (D). Abbreviations: br, branchiostegals; brb, border rostral bones; cl, cleithrum; clv, clavicle; dpt, dermopterotic; drb, dorsal rostral bones; ds1, first dorsal scute; dsp, dermosphenotic; excl, lateral extrascapulars; excm, median extrascapular; fr, frontal; j, jugal; n, nasal; n(t), tubular nasal; pa, parietal; pas, parasphenoid; pfs, pectoral-fin spine; po, postorbital; popcn, tubular ossifications of the preopercular sensory canal; pt, posttemporal; scl, supracleithrum; so, supraorbital, sop, subopercle; vrb, ventral rostral bones.

Figure 6. Skull of *Acipenser stellatus*. Line drawings of A, dorsal, B, lateral, and C, ventral views of the juvenile dermal skull roof, associated bones and pectoral girdle. UMMZ 148980, 160 mm SL. Anterior to left, scale bar equals 10 mm. Abbreviations: br, branchiostegals; brb, border rostral bones; cl, cleithrum; clv, clavicle; dpt, dermopterotic; drb, dorsal rostral bones; ds1, first dorsal scute; dsp, dermosphenotic; excl, lateral extrascapulars; excm, median extrascapular; lrb, lateral rostral bones; ls1, first lateral scute; fr, frontal; icl, interclavicle; j, jugal; n(t), tubular nasal; n, nasal; pa, parietal; po, postorbital; popcn, preopercular sensory canal; pt, posttemporal; rcb, rostral canal bones; scc, scapulocoracoid cartilage; scl, supracleithrum; so, supraorbital; sop, subopercle; vrb, ventral rostral bones.

Figure 7. Skull of *Acipenser stellatus*. Line drawings of A, dorsal, B, lateral, and C, ventral views of the adult dermal skull roof, associated bones and pectoral girdle. VIMS 13552, 235 mm HL. Anterior to left, scale bar equals 10 mm. Abbreviations: an, aortic notch; brb, border rostral bones; dpt, dermopterotic; drb, dorsal rostral bones; ds1, first dorsal scute; dsp, dermosphenotic; excl, lateral extrascapulars; excm, median extrascapular; lrb, lateral rostral bones; fr, frontal; j, jugal; map, median anterior process of the parasphenoid; n(t), tubular nasal; n, nasal; pa, parietal; pas, parasphenoid; po, postorbital; pt(v), ventral lamina of posttemporal; pt, posttemporal; rcb, rostral canal bones; so, supraorbital; sop, subopercle; vrb, ventral rostral bone.

Figure 8. Occipital bones of *Acipenser stellatus*. A, Photograph, and B, line drawing of dorsal view of the posterior portion of the skull roof. UMMZ 148980, 160 mm SL. Anterior to left. Scale bar equals 5 mm. Abbreviations: dpt, dermopterotic; ds1, first dorsal scute; excl, lateral extrascapulars; excm, median extrascapular; llcn, trunk lateral-line sensory canal; ocn, occipital sensory canal; pa, parietal; pt, posttemporal; scl, supracleithrum; sop, subopercle; stcn, supratemporal sensory canal.

Figure 9. Neurocranium of *Acipenser stellatus* in A, dorsal, B, lateral, and C, ventral views. VIMS 13553, 320 mm HL. Bone in light gray, cartilage in dark gray. Anterior to left. Abbreviations: an, aortic notch; arp, ascending ramus of the parasphenoid; btp, basitrabecular process; ctp, central trabecular process; hyf, articulation facet for hyomandibula; lep, lateral ethmoid process; ncap, nasal capsule; os, orbital shelf; pas, parasphenoid; pnw, postnasal wall; ptp, posttemporal process; vrb, ventral rostral bones.

Figure 10. Parasphenoid and ventral rostral bones of *Acipenser stellatus* in A, dorsal, B, lateral, and C, ventral views. VIMS 13552, 235 mm HL. Anterior to left, scale bar equals 10 mm. Abbreviations: an, aortic notch; arp, ascending ramus of the parasphenoid; feba, foramina for efferent branchial arteries; map, median anterior process; pas, parasphenoid; pg, groove on the parasphenoid marking the articulation point with the branchial arches; vrb, ventral rostral bones.

827 **Figure 11.** Opercular bones of *Acipenser stellatus*. Elements in A, lateral, and B, medial views.
828 VIMS 13552, 235 mm HL. Anterior to left in A and to right in B; scale bar equals 10 mm.
829 Abbreviations: br, branchiostegal; sop, subopercle.
830
831 **Figure 12.** Upper jaws of *Acipenser stellatus* in A, dorsal, B, lateral, and C, medial views. VIMS
832 13553, 320 mm HL. Bone in light gray, cartilage in dark gray. Anterior to left, scale bar equals
833 10 mm. Abbreviations: ap, autopalatine; dpl, dermopalatine; ecp, ectopterygoid; plc, palatal
834 complex; ppt, palatopterygoid; pq, cartilage of the palatoquadrate; qj, quadratojugal.
835
836 **Figure 13.** Left lower jaw of *Acipenser stellatus* in A, dorsal, B, lateral, C, ventral, and D,
837 medial views. VIMS 13553, 320 mm HL. Bone in light gray, cartilage in dark gray. Anterior to
838 left in A, B, C, and anterior to right in D, scale bar equals 10 mm. Abbreviations: d, dentary; m,
839 mentomeckelian; mc, Meckel's cartilage; par, prearticular.
840
841 **Figure 14.** Hyoid arch elements of *Acipenser stellatus* in A, lateral and, B, medial views. VIMS
842 13553, 320 mm HL. Bone in light gray, cartilage in dark gray. Anterior to left in A, and anterior
843 to right in B, scale bar equals 10 mm. Abbreviations: cha, anterior ceratohyal; chp, posterior
844 ceratohyal; ehc, external hyomandibular cartilage; ehyc, external hyoid cartilage; h,
845 hyomandibula; h-art, articular head of the hyoid; ihy, interhyal; vhb, ventral hyomandibular
846 blade.
847
848 **Figure 15.** Ventral gill arches (left side) of *Acipenser stellatus* in A, dorsal and B, ventral views.
849 VIMS 13552, 235 mm HL. Bone in light gray, cartilage in dark gray. Anterior to left, scale bar
850 equals 10 mm. Abbreviations: bbc, basibranchial copulae; cb, ceratobranchial; cha, anterior
851 ceratohyal; chp, posterior ceratohyal; hb, hypobranchial, hh, hypohyal.
852
853 **Figure 16.** Dorsal gill arches (left side) of *Acipenser stellatus* in A, dorsal, B, lateral, and C,
854 ventral views. VIMS 13552, 235 mm HL. Bone in light gray, cartilage in dark gray. Anterior to
855 left, scale bar equals 10 mm. Abbreviations: eb, epibranchial; ipb, infrapharyngobranchial; spb,
856 suprapharyngobranchial.
857

Figure 17. Gill rakers (right side) of ventral gill arches of *Acipenser stellatus* in dorsal view. VIMS 13552, 235 mm HL. Anterior to left, scale in mm.

Figure 18. Comparison of the course of the occipital sensory canals in sturgeons. A, *Scaphirhynchus platorhynchus* (VIMS 12098, 250 mm SL); B, *Acipenser fulvescens* (UMMZ 22374, 185 mm SL); C, *Huso huso* (CAS 211810, 130 mm SL); and D, *Pseudoscaphirhynchus hermanni* (VIMS 42683, 182 mm SL). Anterior to left. Abbreviations: dpt, dermopterotic; ds1, first dorsal scute; excm, median extrascapular; excl, lateral extrascapular; llcn, lateral line sensory canal; ocn, occipital sensory canal; pa, parietal; pt, posttemporal; scl, supracleithrum; stcn, supratemporal sensory canal.

Figure 19. Heads of *Pseudoscaphirhynchus* species in left lateral view showing variation in cranial spines. A, *P. kaufmanni* (ZMMU P-1456,171 mm SL); B, *P. kaufmanni x P. hermanni* hybrid (UAIC uncataloged, 211 mm SL); C, *P. hermanni*, short-snouted morph (UAIC uncataloged , 169 mm SL); D, *P. hermanni*, long-snouted morph (ZMMU P-1904, 157 mm SL); E, *P. fedtschenkoi*, short-snouted morph (ZMMU P-640, 185 mm SL); and F, *P. fedtschenkoi*, long-snouted morph (ZMMU P-640, 195 mm SL). Scale bars equal 20 mm.

Figure 20. Heads of species of *Huso* and *Acipenser* in left lateral view showing variation in cranial spines. A, *H. dauricus* (ZMMU P-7707, 352 mm SL); B, *A. sturio* (ZMMU P-13015, 318 mm SL); C, *A. baerii* (ZMMU uncataloged; 228 mm SL); D, *A. ruthenus* (ZMMU P-1987, 199 mm SL); E, *A. schrenki* (ZIN 17934, 251 mm SL); F, *A. nudiventris* (ZIN 4508, 352 mm SL); G, *A. colchicus* (MHNH 1925-54; 207 mm SL); H, *A. colchicus* (MNHN 1901-120; 746 mm SL). Scale bars equal 20 mm.

Figure 21. Head of *Scaphirhynchus platorhynchus* in left lateral view showing cranial spines (VIMS 13515, 570 mm SL). Insets at the top show enlargements of spines (indicated by white arrows) at the tip of the snout (left) and the posterior portion of the skull roof (right). Anterior facing left. Scale bar equals 20 mm.

Table 1. Summary of morphometric data of the head for a sample of Acipenser stellatus.

	n	Minimum	Maximum	Average
As % Standard Length (SL)				
Head Length (HL)	38	27	39	32
As % HL				
Preorbital Length	40	51	68	61
Prenares Length	40	38	61	53
Preoral Length	40	55	76	68
Prebarbel Length	40	30	53	44
Skull Width at Opercular Flap	40	19	33	27
Interorbital Width	40	14	27	23
Head Width at Nares	40	20	33	25
Head Width at Barbels	40	16	28	21
Mouth Width	38	12	24	14
Head Height at Opercular Flap	40	23	35	29
Head Height at Orbit	40	16	28	21
Head Height at Nares	40	9	20	15
Head Height at Barbel	39	7	13	10

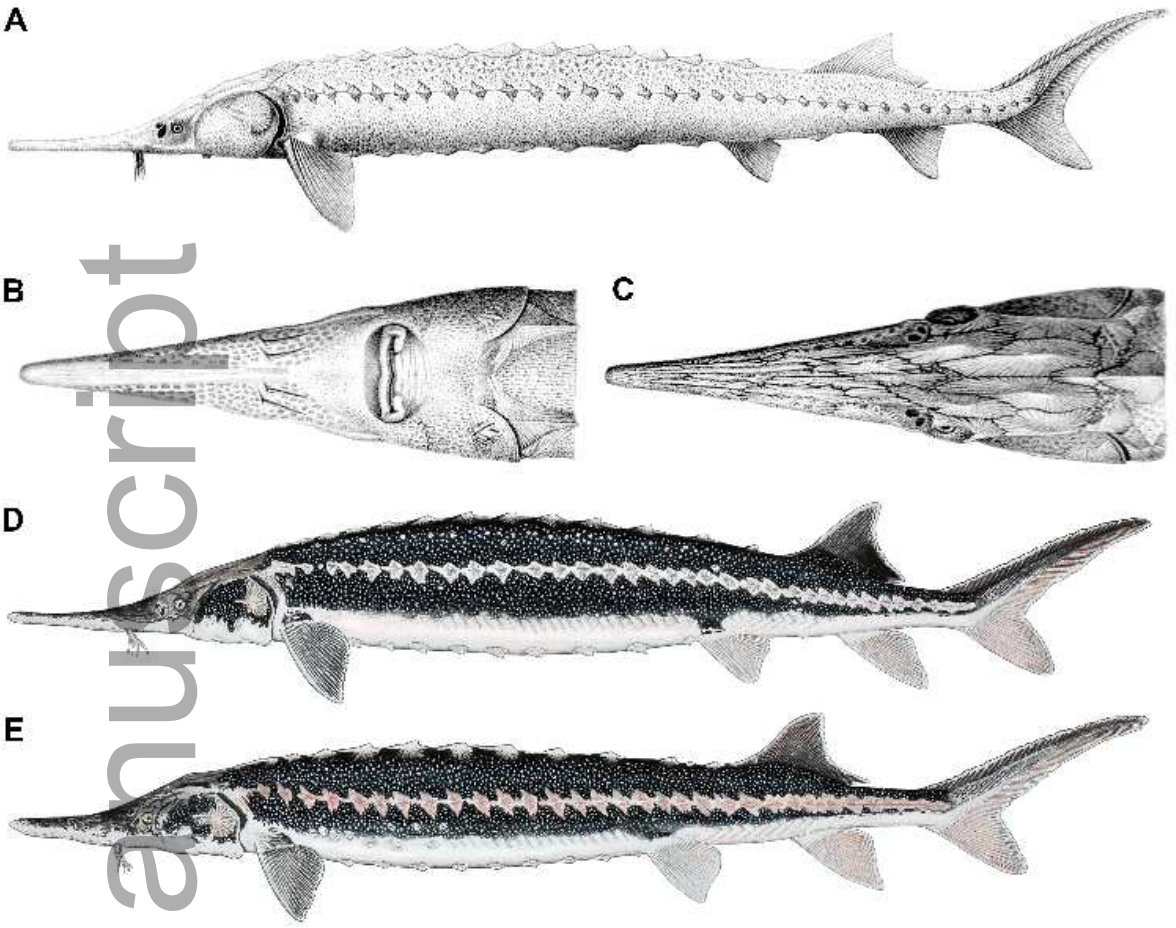

azo_12355_f1.jpg

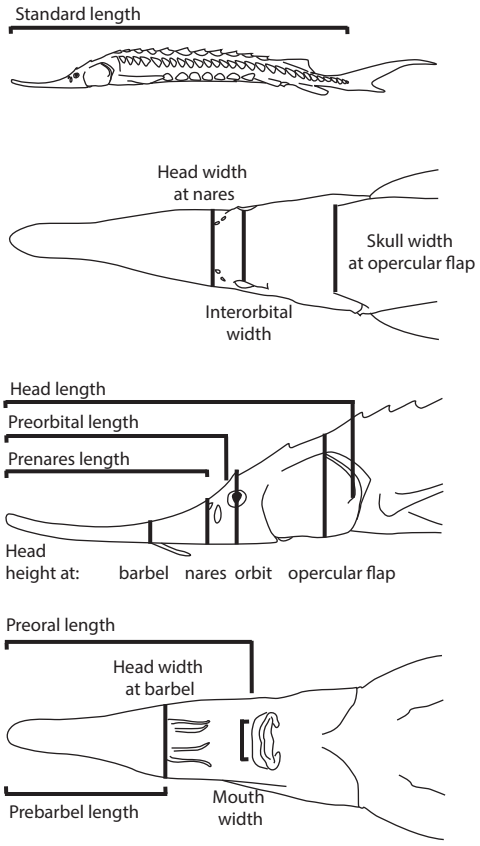

azo_12355_f2.ai

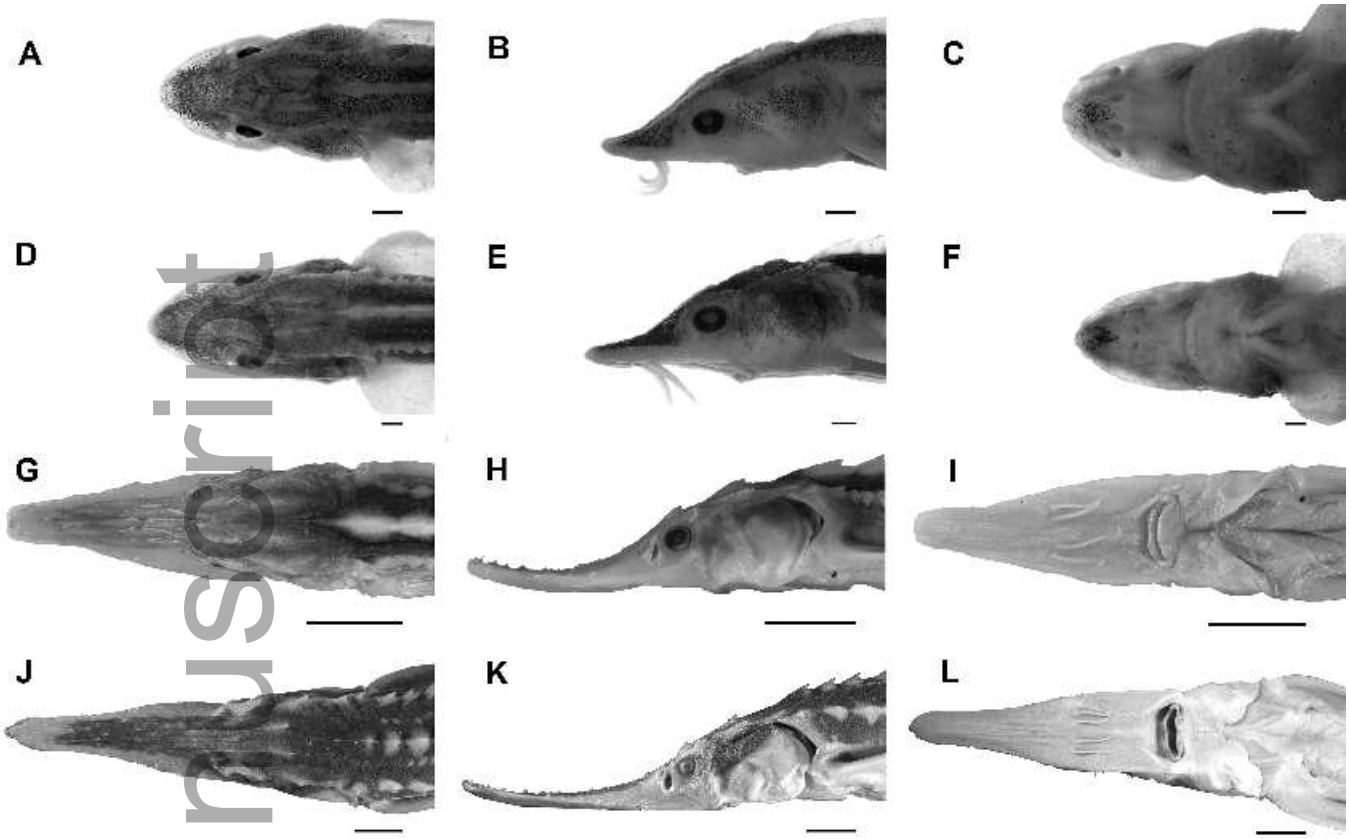

azo_12355_f3.jpg

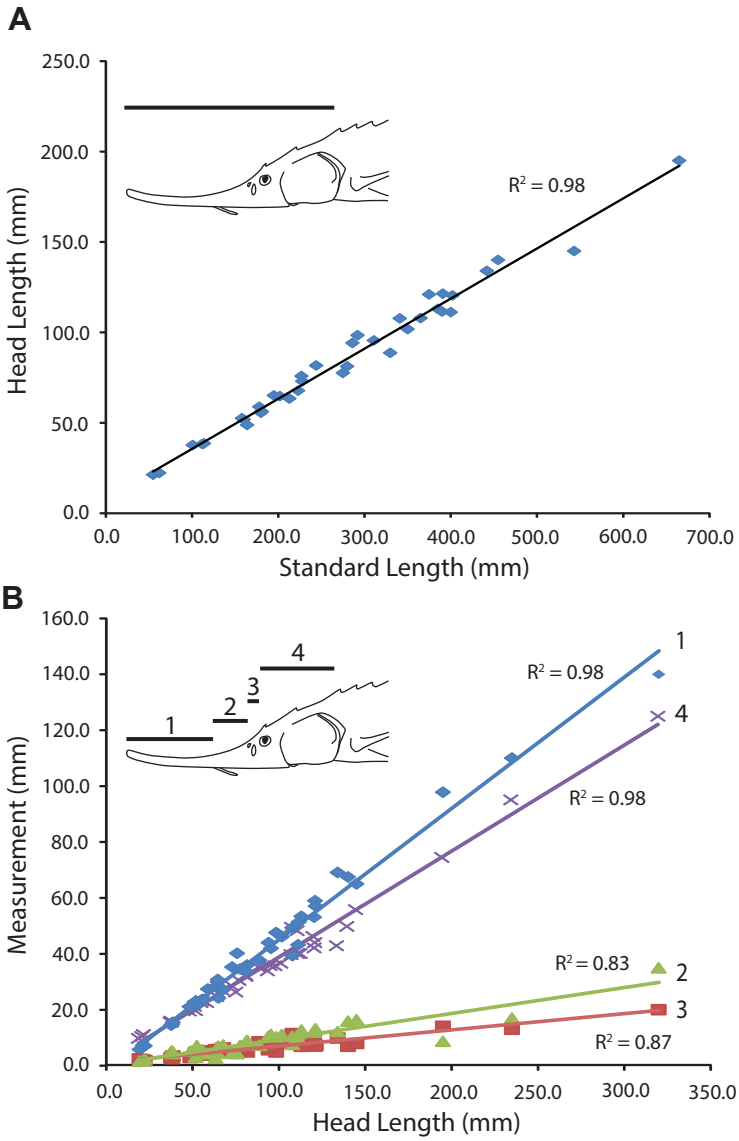

azo_12355_f4.ai

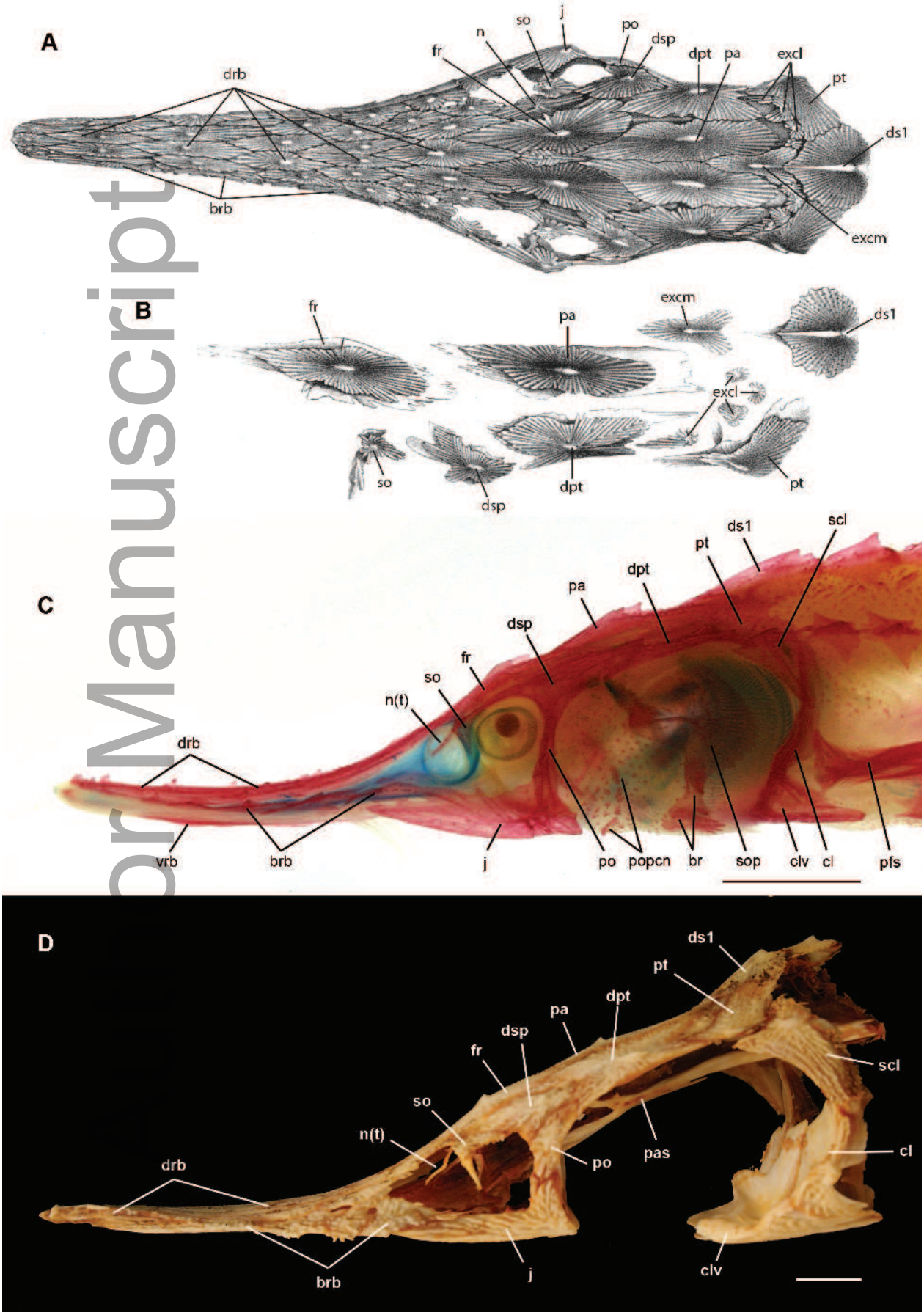

azo_12355_f5.tif

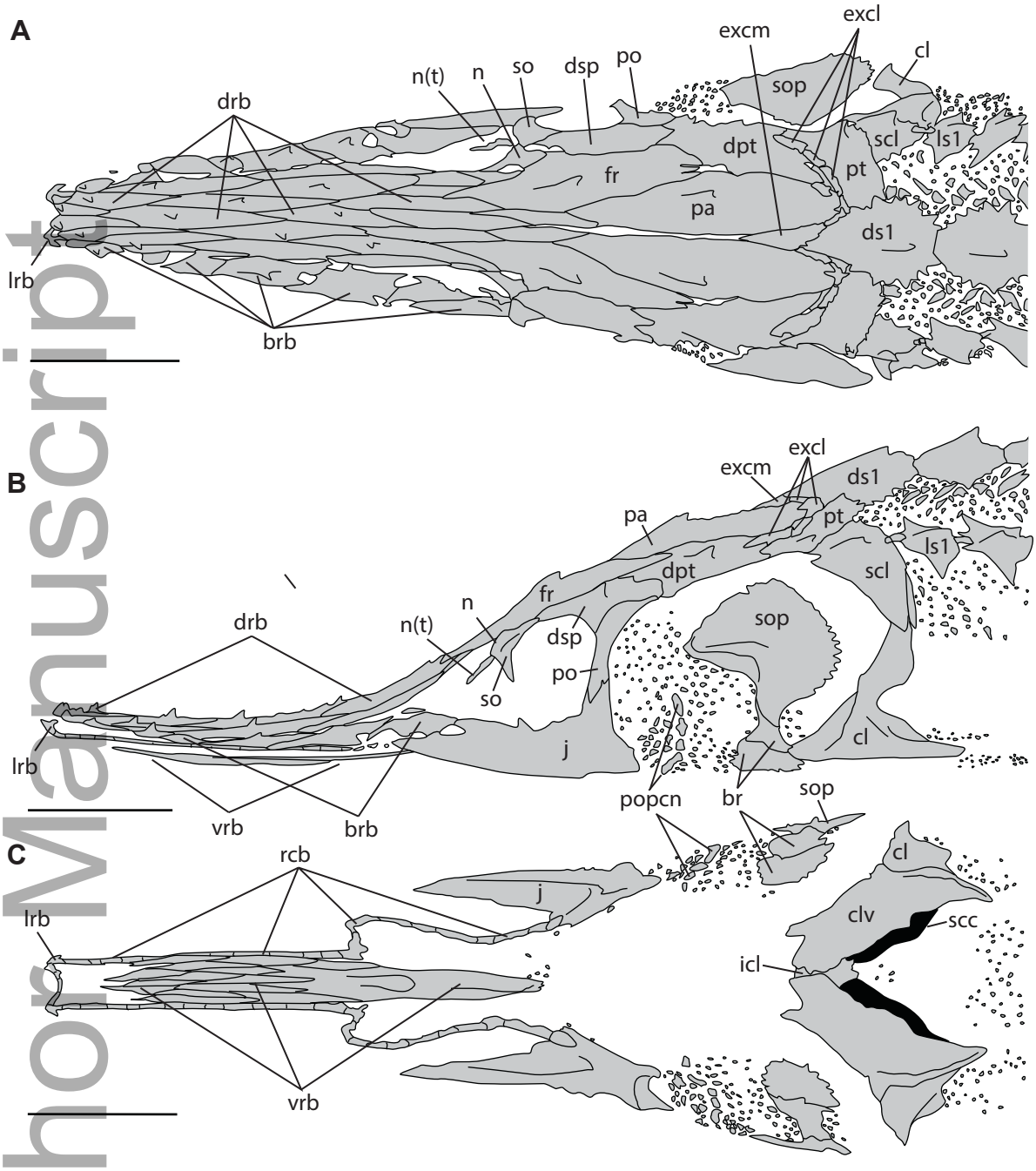

azo_12355_f6.ai

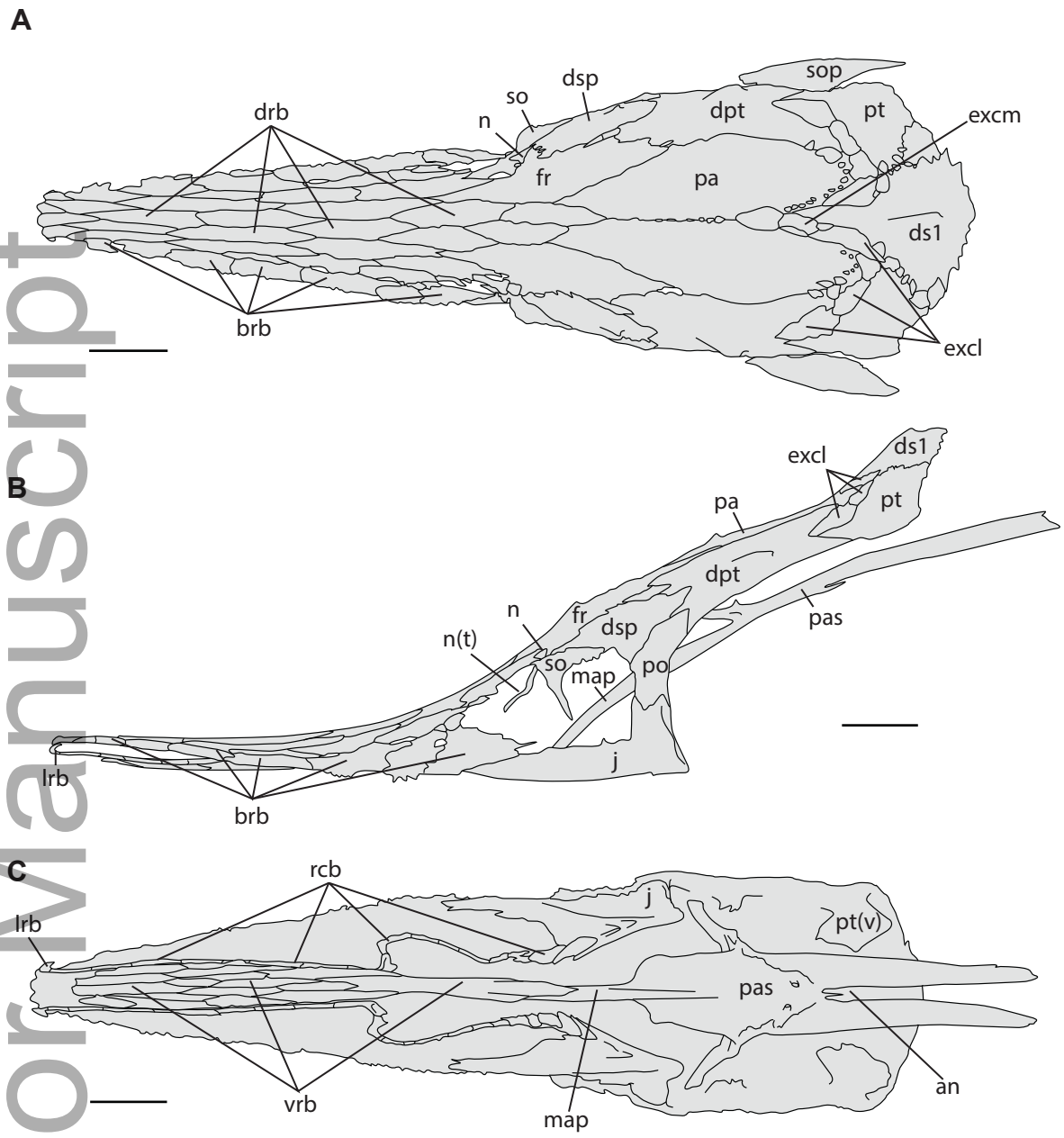

azo_12355_f7.ai

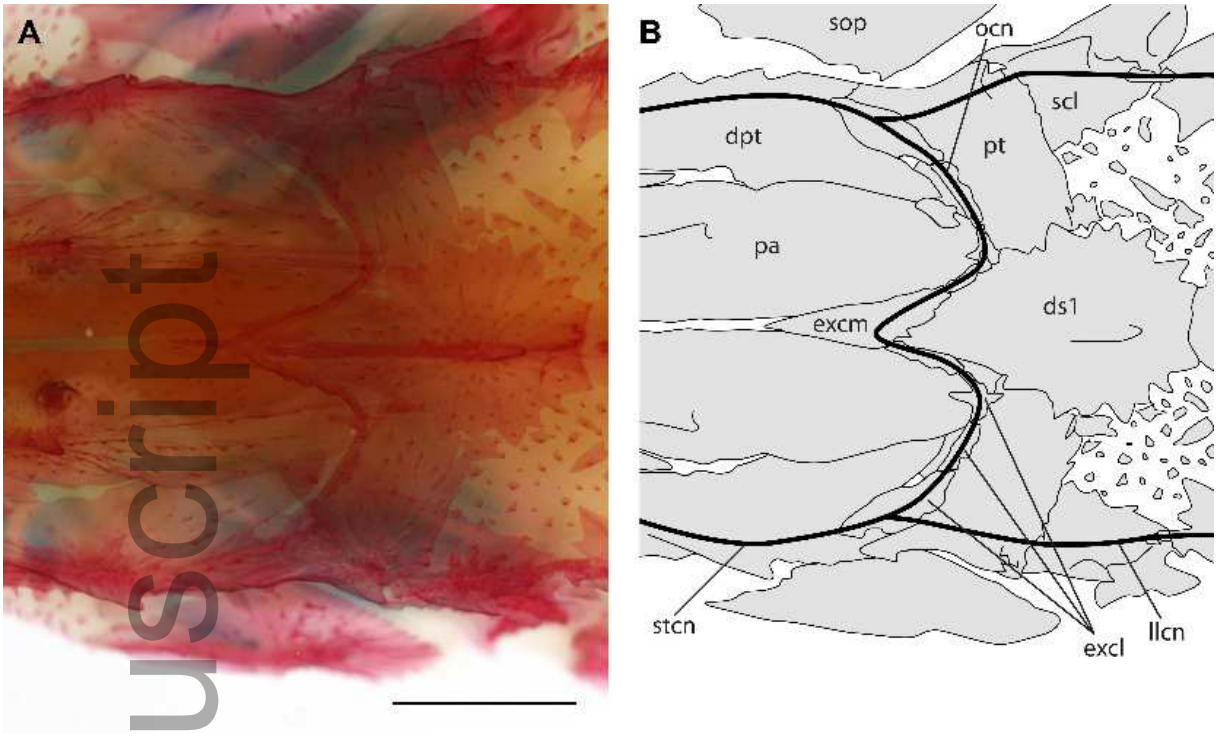

azo_12355_f8.jpg

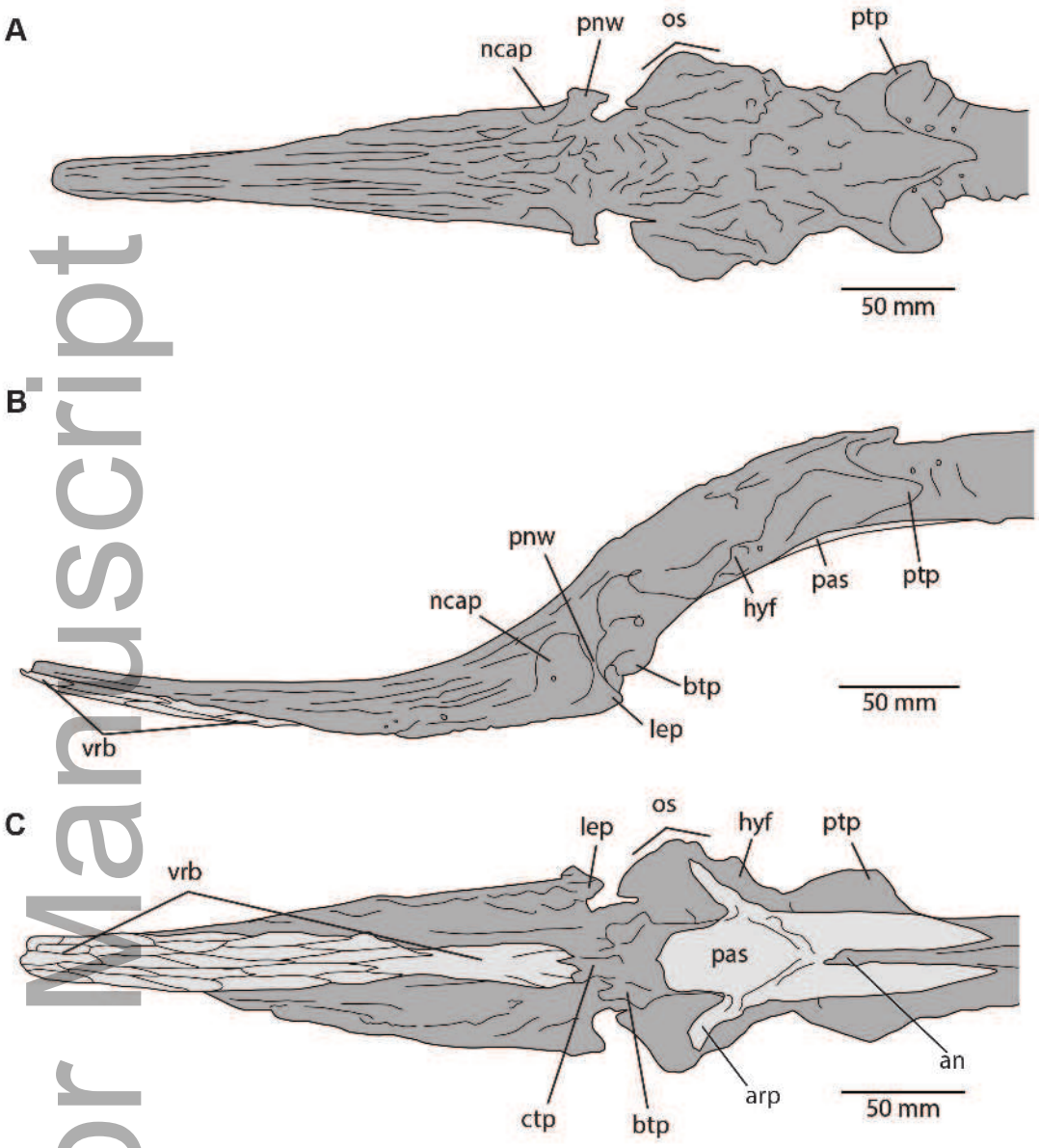

azo_12355_f9.jpg

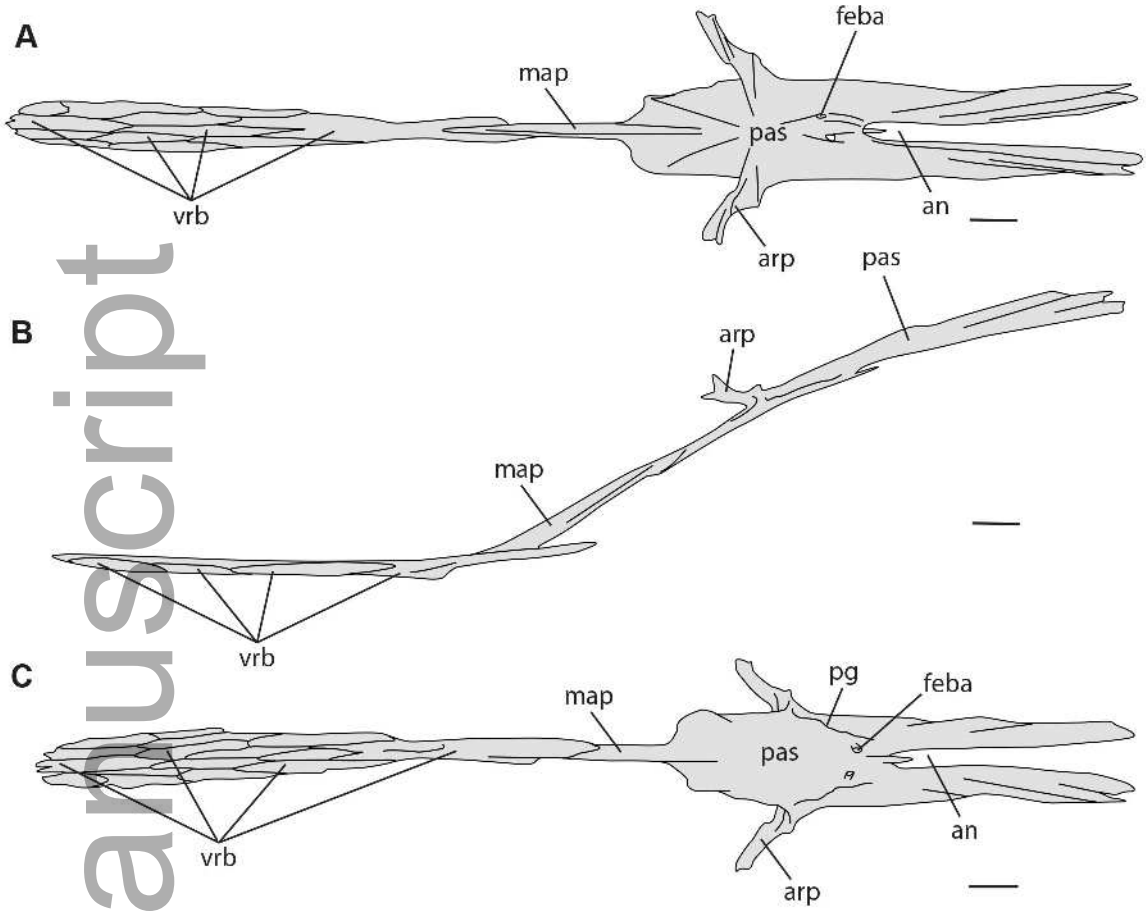

azo_12355_f10.jpg

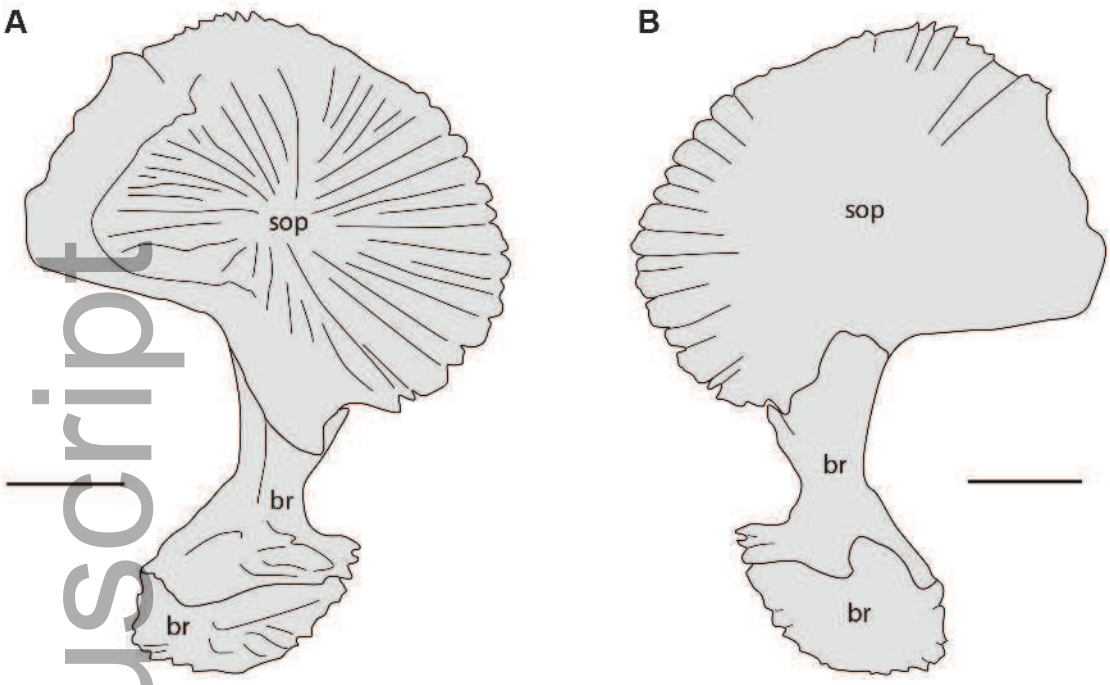

azo_12355_f11.jpg

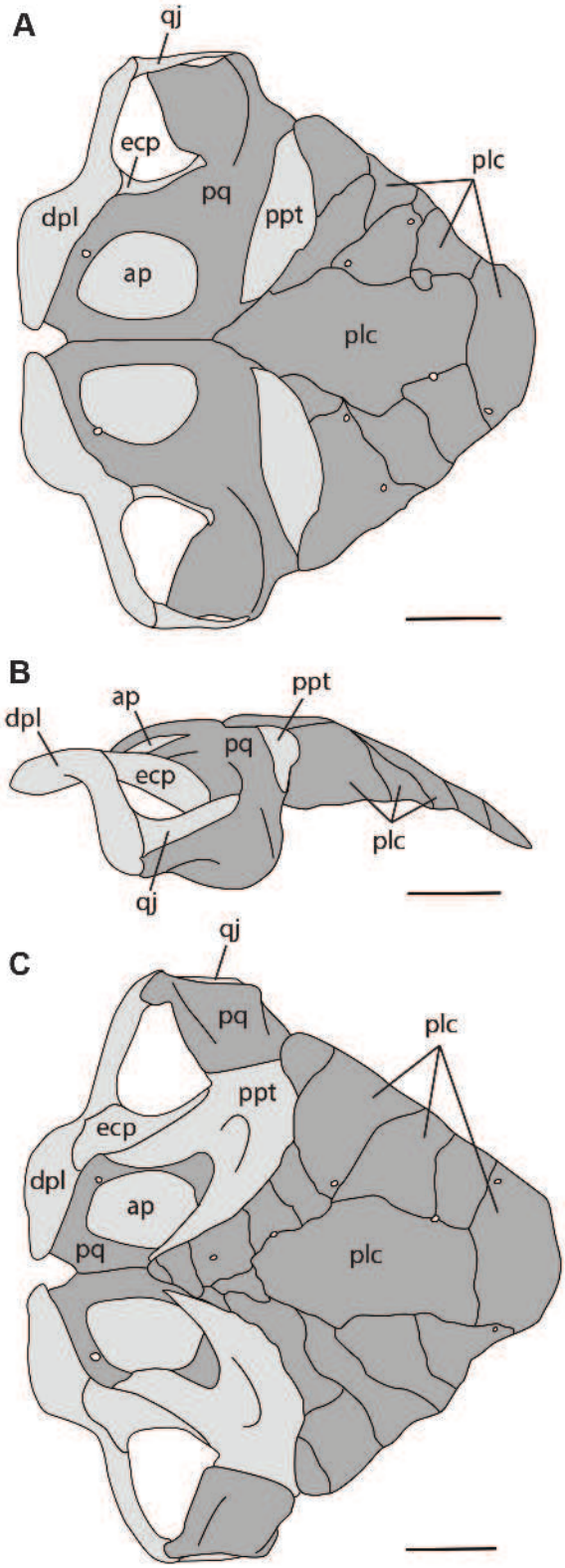

azo_12355_f12.jpg

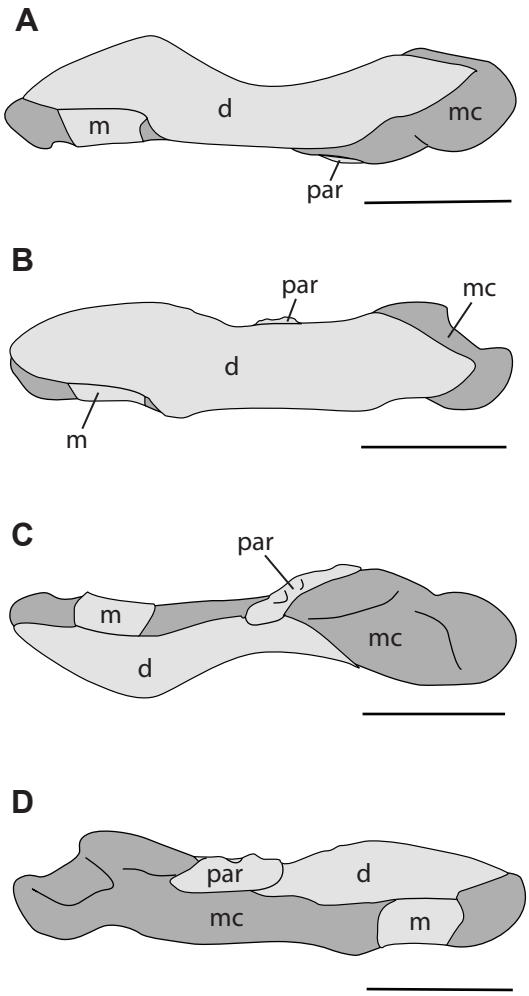

azo_12355_f13.ai

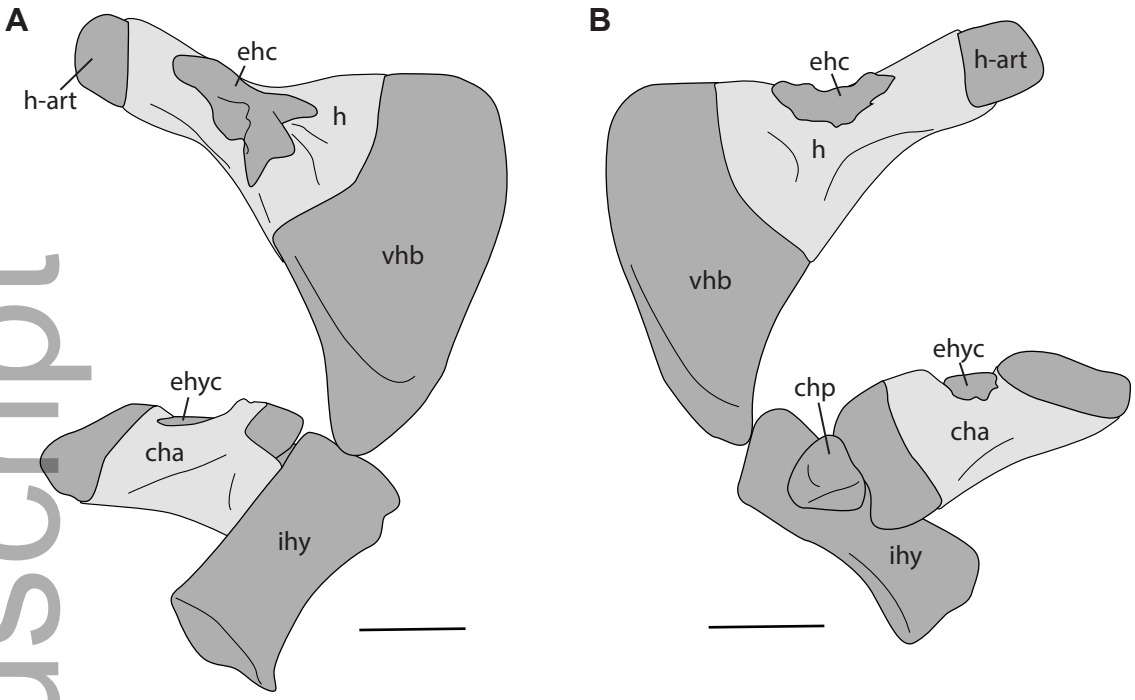

azo_12355_f14.ai

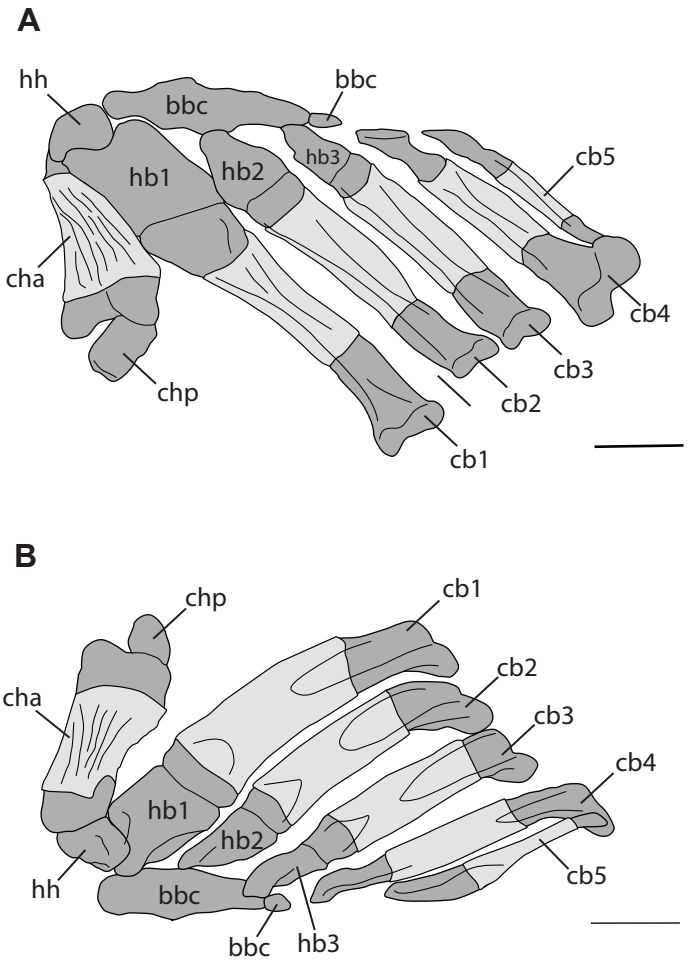

azo_12355_f15.ai

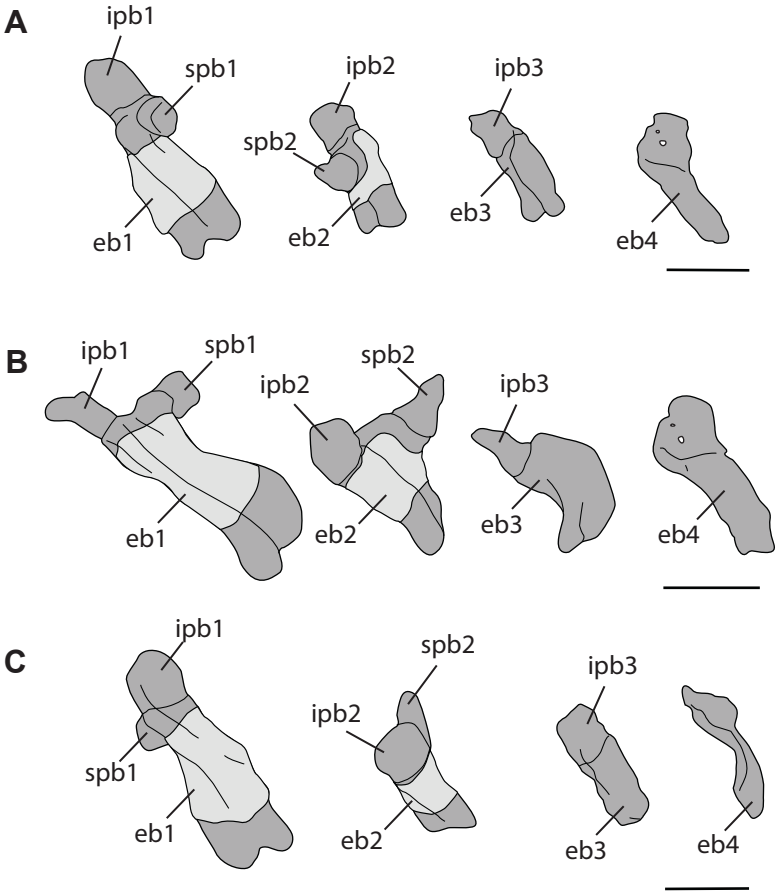

azo_12355_f16.ai

azo_12355_f17.tif

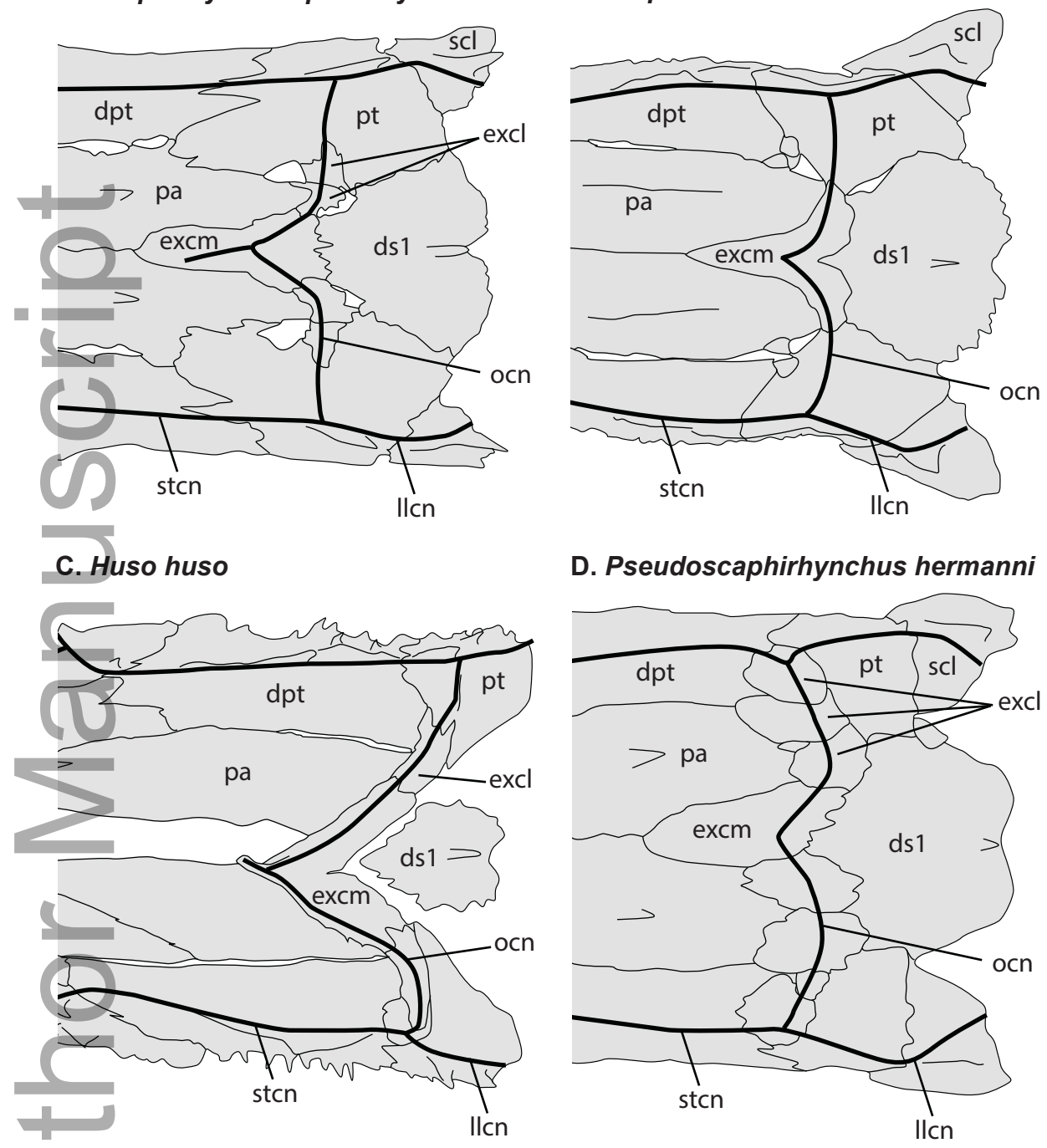

azo_12355_f18.ai

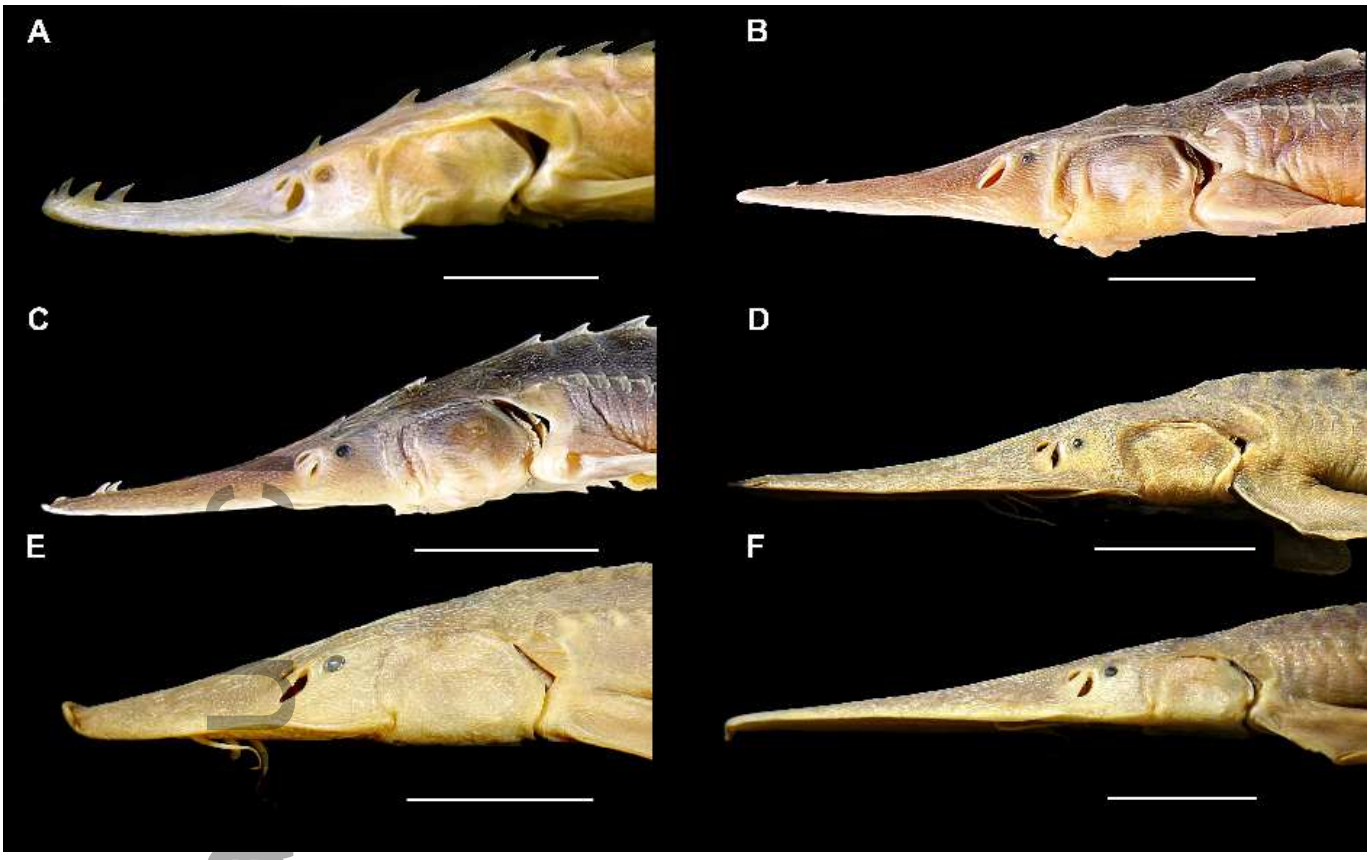

azo_12355_f19.jpg

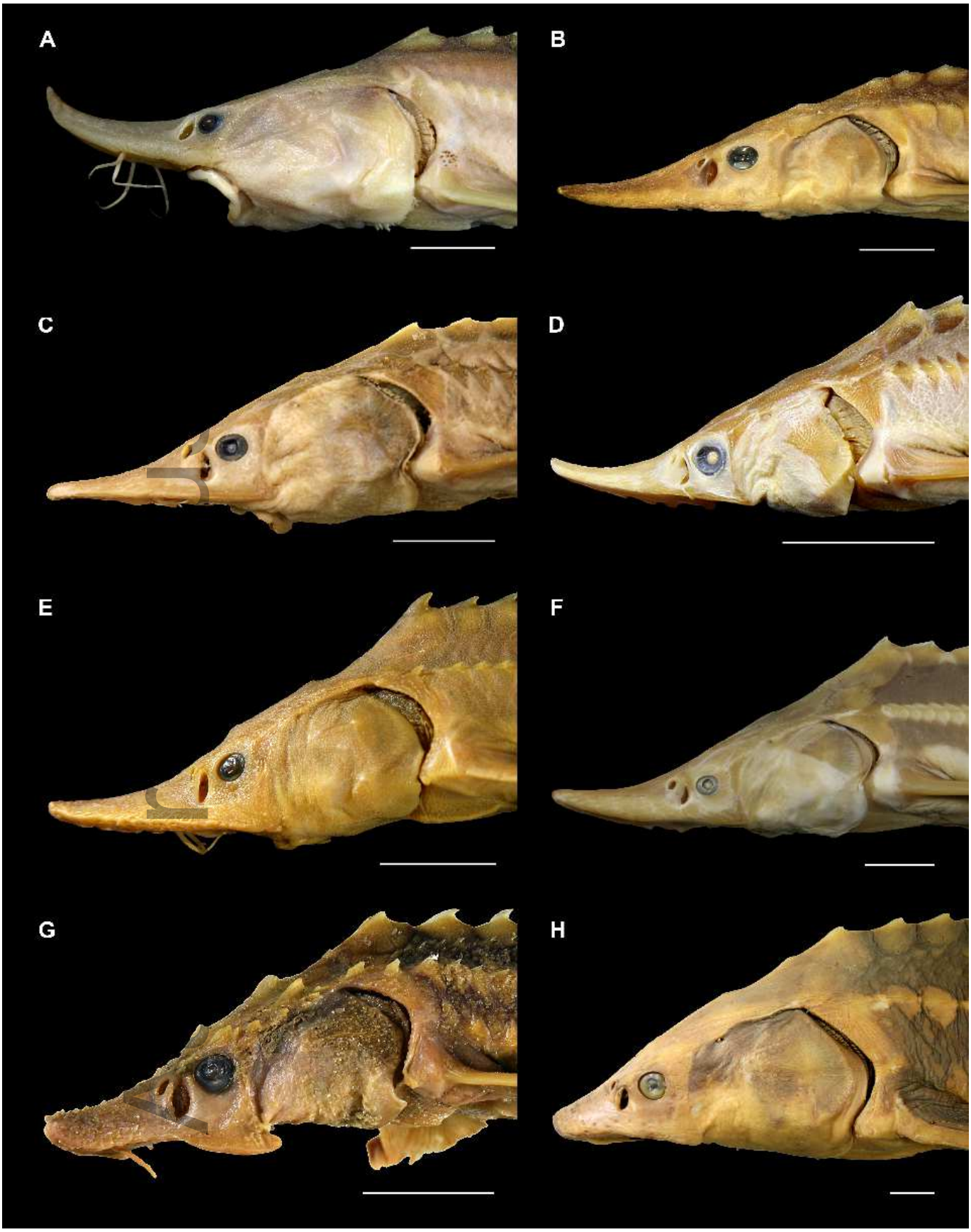

azo_12355_f20.jpg

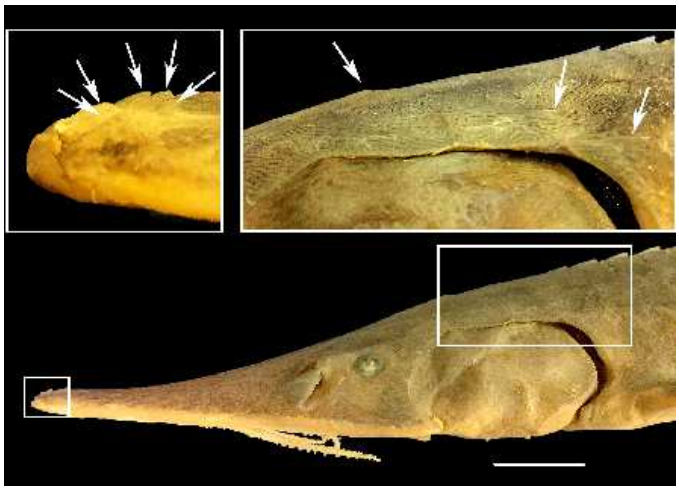

azo_12355_f21.jpg